Effect of Different Treatment Methods on the Interfacial Transition Zone Microstructure to Coarse Recycled Concrete Aggregate

Hanaa Khaleel Alwan Al-Bayati[1]

Ph.D. Candidate, Centre for Pavement and Transportation Technology (CPATT), Department of Civil and Environmental Engineering, Faculty of Engineering, University of Waterloo, 200 University Avenue West, Waterloo, Ontario, Canada N2L 3G1,
Phone: +1-519-888-4567× 30187 , Fax: +1-519-888-4300, E-mail: halwan@uwaterloo.ca

Susan L. Tighe

Ph.D., P. Eng., Professor, Norman W. McLeod Professor of Sustainable Pavement Engineering, Director of Centre for Pavement and Transportation Technology (CPATT), Department of Civil and Environmental Engineering, Faculty of Engineering, University of Waterloo, 200 University Avenue West, Waterloo, Ontario, Canada N2L 3G1, Phone: +1-519-888-4567× 33152,
Fax: +1-519-888-4300, E-mail: sltighe@uwaterloo.ca

Hassan Baaj

Ph.D., P. Eng., Associate Professor, Norman W. McLeod Professor in Pavement Materials, Centre for Pavement and Transportation Technology (CPATT), Department of Civil and Environmental Engineering, Faculty of Engineering, University of Waterloo, 200 University Avenue West, Waterloo, Ontario, Canada N2L 3G1, Phone: +1-519-888-4494,
Fax: +1-519-888-4300, E-mail: hbaaj@uwaterloo.ca

Principal Author: Hanaa Khaleel Alwan Al-Bayati

Paper prepared for presentation at

the GREEN TECHNOLOGY IN GEOTECHNICAL AND MATERIALS ENGINEERING Session

of the 2016 Conference of the

Transportation Association of Canada

Toronto, ON

[1] Lecturer in Civil Engineering Department, College of Engineering, University of Tikrit, Tikrit, Iraq

Abstract

Sustainability and awareness of the environment are increasingly becoming important for transportation agencies worldwide. In Canada, many agencies are interested in maximizing the use of recycled materials into roads. The main objective of this investigation study is to examine the effect of different treatment methods on Coarse Recycled Concrete Aggregate (CRCA) for usage in roads. One of the key material properties related to using CRCA is the interfacial transition zone (ITZ). ITZ characteristics particularly microcracks and intermix phases on both sides of ITZ are calculated. Mortar properties including pore size and matrix (macro) cracks properties: width, length and crack density are also examined. Heat treatment includes various temperatures (250ºC, 350ºC and 500ºC). Pre-soaking method involves the use of strong acid HCl and weak acid $C_2H_4O_2$. In order to achieve surface characterization of the ITZ region and CRCA surface of both of the treated and untreated CRCA, different advanced techniques are used such as Scanning Electron Microscopy (SEM) and Energy Dispersive X-ray Microanalyzer (EDAX). The obtained results revealed that the use of heat treatment is highly successful in improving properties of microcracks ITZ including width and length of microcracks. Heat treatment at 250°C exhibits the best performance by considerably decreasing the Ca/Si ratio resulting in big transformations for aggregate side, whereas the optimum behavior for mortar side improvement is recorded at 350°C. A successful acid treatment is recorded for both types; strong and weak acid for decreasing pore size and lowering width and length of the ITZ microcracks. However, the weak acid appears to be more successful in terms of improving the mortar in the ITZ, whereas the strong acid is more effective on the aggregate. The outcomes also indicated that there is a positive influence with the heat treatment at a temperature range between (0-350°C) on lowering pore size, whereas various negative impacts are observed at higher temperatures including width and length of matrix cracks and pore size. The crack density on the mortar side is highly related to properties of matrix cracks including width and length though behavior of properties is completely different.

Keywords: Coarse Recycled Concrete Aggregate (CRCA), Heat treatment, Acid treatment, Interfacial Transition Zone (ITZ), Microcracks, Matrix cracks, Ca/Si ratio

1. Introduction

Among various types of construction materials, concrete, being the most extensively consumed material, is responsible for rapid depletion of natural resources as a significant amount of its main constituent materials, especially aggregates, are drawn from nature (Mukharjee & Barai, 2014). According to the Ontario Ministry of Natural Resources (MNR), the average consumption of aggregate reached approximately 179 million tonnes per year in Ontario during the period of 2000-2009, while this average is projected to amount approximately 191 million tonnes between 2020 and 2029 (MNR, 2010). Therefore, this would lead to critical shortage of natural aggregates in Ontario and similarly in other Canadian provinces and in other countries worldwide. Additionally, the manufacturing process of concrete and its main constituent, the Portland Cement (PC), releases massive amounts of various pollutants including carbon dioxide, sulfur compounds and nitrogen compounds that are responsible for serious environmental pollution (Mukharjee & Barai, 2014). For instance, the manufacture of one ton of Portland Cement leads to the release of nearly one ton of carbon dioxide into the environment depending on the production process type (Demie et al., 2013).

Simultaneously, tremendous amounts of construction and demolition waste are generated from various activities including construction, renovation, and demolition of aged buildings and civil engineering structures. Recently, the amount of construction and demolition waste generated was estimated annually at 1,183 million tonnes worldwide (Purushothaman et al., 2014). The control and management of these huge waste quantities is becoming a serious challenge worldwide especially for large urbanized areas due to the continuous increase of waste quantities, lack of sufficient landfills for dumping of waste materials, and cost increases in transportation and disposal. Therefore, the current practices of the construction industry would be considered is environmentally unfriendly and unsustainable.

All these factors highlight the urgent need to identify innovative ways of recycling and reusing waste materials. In order to dispose of the tremendous amounts of construction and demolition (C&D) wastes, to reduce the consumption of natural aggregate resources and to reduce the carbon footprint of the concrete industry, an environmentally friendly and sustainable construction material, recycled concrete aggregate (RCA), was developed to be a green solution to these problems (Zhang et al., 2015).

2. Literature review:

Concrete is a highly complex, heterogeneous and multiphase composite material at the microstructural level, consisting of three main phases: aggregate, bulk cement paste (matrix) and an interfacial transition zone (ITZ) between the aggregates and the matrix (Otsuki et al., 2003; Akçaoğlu et al., 2005; Tam et al., 2005; Tam & Tam, 2008; Tam et al. 2007; Xuan et al. 2009; Kong et al., 2010; Erdem et al., 2012; Li et al., 2012; Erdem et al., 2012). Among the constituents, the ITZ, which is structurally and mechanically different from the matrix and aggregate, is essentially composed of three phases, namely: water film, $Ca(OH)_2$ (CH) crystals layer and porous paste matrix layer (Wong et al., 2009; Erdem et al., 2012; Jawahar et al., 2013).

Though the origin of the ITZ has not been fully understood yet, the common view for the existence of the ITZ is namely titled the “wall effect”. This potential mechanism briefly refers to spatial arrangements of anhydrous cement particles against an aggregate surface due to size discrepancy. More specifically, it is well known that the typical size of cement particles range between (1-100μm), whereas the average size of aggregate is predominantly many times larger than that of cement particles. In freshly compacted concrete, the cement particles are suspended and its normal packing is disrupted. The cement particles cannot pack effectively when they are close to large solid objects, such as aggregates due to the phenomenon of the creation of a geometric wall effect within the structure which results creating a narrow region around the aggregates, namely the ITZ. The region is characterized by a relatively low concentration of cement particles, high water content and consequently increased porosity (Cwirzen & Penttala, 2005; Leemann et al., 2006; Wang et al., 2009; Gao et al., 2014; Sun et al., 2015; Wu et al., 2016).

As with other composite materials, the properties of the concrete are highly dependent on the properties of each individual component, especially the connection area between major components, and concrete properties are considerably determined by the ITZ (Akçaoğlu et al., 2005; Li et al., 2012). It has been widely reported that the ITZ is a weak region (Otsuki et al., 2003; Tam et al., 2005; Tam et al., 2007; Poon et al., 2006; Duan et al., 2013) due to a high presence of voids and microcracks that are highly related to strength properties. Subsequently, the ITZ plays a crucial role for determining the mechanical performance of concrete (Tam et al. 2005; Tam et al. 2007; Güneyisi et al., 2014), though it is generally thin, between 10-50 µm (Kong et al., 2010). Therefore, the improvement of RCA microstructure has been a considerable concern that noticeably interested many researchers and compelled them to enhance the characteristics of the concrete (Kong et al., 2010; Jawahar et al., 2013; Purushothaman et al., 2014). However, the factors that play an important role for forming the structure of the ITZ and its properties are the aggregate properties including type, shape and surface conditions, cement and admixtures and particularly the water-to-cement (w/c) ratio of the mixture (Akçaoğlu et al., 2005). Figure 1 represents a schematic diagram for the ITZ zone.

Though the matrix and aggregate properties have an important effect on crack initiation and propagation, the ITZ properties have a considerable and particular importance with regards to the cracking of concrete (Akçaoğlu et al., 2005). From the literature, it was concluded that the main reason for initial microcracks is the large difference between the modulus of elasticity of the aggregate and the matrix, resulting in higher tangential, radial and/or shear stresses at the interface zone (Akçaoğlu et al., 2005; Jawahar et al., 2013). The microcracks can be mainly classified as either bond cracks or matrix cracks. The bond cracks typically initiate and appear at the interface zone, whereas matrix cracks generally propagate across the cement paste (Jawahar et al., 2013). However, the typical width of microcracks ranges between 0.5 and 10 µm (Wong et al., 2009). During concrete loading, increased concentration of microcracks makes them behave as sources of subsequent macrocrack development that includes ITZ microcracks growing through the matrix and combining with the matrix cracks to form macrocracks (Akçaoğlu et al., 2005).

Numerous studies focused on the addition of pozzalanic materials such as fly ash and silica fume as a way for enhancing microstructure, especially the ITZ region of RCA. Tam and Tam (2008) developed two mixing approaches namely two-stage mixing approach (silica fume) and two-stage mixing approach (silica fume and cement). The first approach includes the addition of silica fume into percentages of Recycled Aggregate (RA) in the first mix, whereas the second technique consists of the addition of silica fume and amounts of cement into particular proportions of RA in the first mix. The results of both techniques revealed that the utilization of silica fume and proportional cement percentages lead to filling up the weak areas in the RA, resulting in an improved interfacial region and higher strength of the concrete. Comparable outcomes were noted by other researches (Tam et al., 2005; Li et al., 2009; Li et al., 2012) who investigated enhancing RCA properties and microstructure through using a two stage mixing approach. The studies concluded that there is an improvement in the ITZ region and RCA properties by using this approach. Compared with the double mixing method it was revealed that there is a further improvement for the ITZ and RCA properties through using a triple mixing method. The technique includes surface coating of RCA with materials such as fly ash and silica fume. The captured images of SEM analysis indicated that the coated pozzolanic particles can consume CH particles that are accumulated in the pores and on the surface of the attached mortar to form new hydration products resulting in successful improvement in ITZ microstructure and enhanced strength of RCA (Kong et al., 2010).

The effect of different coarse RCA on the ITZ was examined on six different sources of coarse RCA with varying strengths and quantities of attached mortar. The obtained results demonstrated that there is a significant influence of the quality of attached mortar on ITZ properties. However, it was observed that there is no obvious impact of the quantity of attached mortar on ITZ properties (Otsuki et al., 2003). Poon et al. (2004) investigated the influence of RCA types on microstructure of ITZ of concrete mixes prepared with RCA. Two different types of RCA including recycled normal strength concrete (NC), and recycled high performance concrete (HPC) with water absorption 8.82% and 6.77% were respectively used in concrete mix design with a constant water to cement ratio of 0.5 for both concrete mixes. The outcomes of SEM images showed that the ITZ of NC mix mainly consists of loose and porous hydrates, whereas the ITZ of HPC mix is fundamentally composed of dense hydrates. The adverse influence of attached mortar on self-compacting concrete (SCC) containing RCA through using surface treatments was investigated. Various surface treatment methods were applied including a two-stage mixing approach, pre-soaking in HCl solution, water glass dispersion and cement–silica fume slurry. The captured images of SEM analysis revealed that the new ITZs with treated RCA by using the two stage mixing approach, water glass and HCI solution are characterized by less porous, highly dense and connected microstructure compared to untreated RCA due to the recovery of microcracks and voids in RCAs. In contrast, the use of cement–silica fume treatment resulted in porous microstructure and weaker bonding in the new ITZ. Among different surface treatments, a considerable improvement to the ITZ was recorded for the two stage mixing approach through providing a layer of cement slurry on the surface of RCA which fills up the microcracks and voids (Güneyisi et al., 2014).

While thoroughly examining the literature related to methods and techniques of RCA treatments and microstructure studies of RCA, it was clearly observed that there is a considerable lack of knowledge on the effects of RCA treatments on ITZ properties, in particular, microcrack and macrocrack development. The previous literature investigations have extensively highlighted the effects of various treatment types on the enhancement of physical properties of RCA, resulting in an obvious gap in this area. Therefore, this research particularly focused on studying the effect of various treatments on enhancing ITZ properties through examination of ITZ microcracks.

3. Research objective

The main objective of this research was to investigate the influence of different treatment methods on ITZ properties in particular of microcracks for coarse recycled concrete aggregate (CRCA). Additionally, attached mortar properties including macrocracking behavior and development, crack density and pore size due to various treatments were examined.

4. Materials and methods

4.1 Materials

The RCA material is classified as a granular A according to the Ontario Provincial Standard Specifications (OPSS.MUNI 1010). The RCA was produced by Steed and Evans Ltd in the Region of Waterloo, Ontario. In this study, the CRCA is defined as the sieve fraction retained between 4.75 and 19 mm. The results of physical properties of CRCA are shown in Table1.

4.2 Methods

4.2.1 Treatment methods of CRCA

The CRCA was washed thoroughly, then dried in an oven at 105±5°C for 24 hours before being used for different types of treatments and tests. The CRCA was soaked in an acidic solution composed of Hydrochloric acid (HCl) (37%) and Acetic acid ($C_2H_4O_2$) (99.7%) obtained from Sigma-Aldrich at a low concentration of 0.1 M for 24 hours at room temperature around 20°C. The CRCA was submerged in distilled water and drained to remove acidic solution, then the samples were dried at 105±5°C for 24 hours to prepare for testing, whereas heat treatment was conducted at different temperatures: 250°C, 350°C and 500°C for a period of one hour in a conventional electric oven.

4.2.2 Measurement of microcracks for ITZ zone

The ITZ microcracks for CRCA were investigated at the Waterloo Advanced Technology Laboratory in the Chemistry Department at the University of Waterloo by using Scanning Electron Microscopy (SEM) (Zeiss Ultra plus microscope) at various working distances and magnification factors.

4.2.3 Measurement of elemental composition for both sides of ITZ

In order to achieve the research objective, the SEM was fit with an energy dispersive X-ray (EDX) spectrometer for scanning the regions of aggregate and mortar sides to examine elemental composition. The specimens of approximate size 10 mm were prepared, dried and coated with a thin layer of gold. The specimens were analyzed under an accelerating voltage of 20 kV of energy at various working distances and magnification factors for SEM analysis, whereas EDAX samples were examined at an accelerating voltage of 20 kV and 100 magnification.

4.2.4 Characterization of intermix phases

In order to distinguish intermix hydrate phases rich in calcium-silicate hydrate C-S-H, high calcium hydroxide (CH) and monosulfate (AFm), the following classification was used in this investigation (Trägárdh 1999; Erdem et al., 2012):

$CSH\colon\ 0.8 \le Ca/Si \le 2.5, (Al + Fe)/Ca \le 0.2$

$CH\colon\ Ca/Si \ge 10, (Al + Fe)/Ca \le 0.4$

$AFM\colon\ Ca/Si \ge 4, (Al + Fe)/Ca > 0.4$

4.2.5 Measurement of matrix (macro) cracks density and pore size

The length and width of macrocracks, and pore size for the mortar surface was obtained from captured images of SEM analysis. The macrocrack density (1/μm), equal to the macrocrack length per area unit, was calculated by dividing the total length of the macrocrack (μm) by the total examined surface area (μm2).

5. Results and discussion

5.1 Influence of treatment types on ITZ microcracks (interface gap)

The differences between the microstructure of ITZs for untreated and treated CRCA were studied using the images indicated in Figures (3-8). The magnified perspectives shown in Figure

3 show the captured image of untreated CRCA with a microcrack interface (gap interface) between the aggregate and attached mortar. It is demonstrated that the microcrack width is not uniform in the ITZ microstructure as it was reported by previous investigations (Jawahar et al., 2013). Instead, the maximum width of the microcrack is 129.7μm, which represents between 2-3 times the usual thickness of ITZ for a concrete or recycled concrete material. The size of the microcrack can be responsible for increasing ITZ porosity, decreasing interface bonding and making this area weaker than the surface of both mortar and aggregate. Therefore, this observation will be very helpful to understand ITZ properties and it should be considered through investigation of strength of recycled concrete. However, there is no mention about this observation in the literature related to concrete and recycled concrete according to the best of the authors' knowledge.

In order to understand behavior of the width and length of microcracks in the ITZ, the maximum width and length of microcracks for acid treatment types are tabulated in Table 2. The obtained results of heat treatment under different conditions are graphically analyzed in Figure 2. Overall, it is clearly noticeable that there is a considerable reduction in width and length of microcracks resulting in a significant improvement to the ITZ. This is mainly attributed to a large accumulation of Calcium Silicate Hydrate (CSH) particles, which result from various reactions as in the following equations:

$$2Ca_3SiO_5 + 6H_2O \rightarrow 3CaO.2SiO_2.3H_2O + 3Ca(OH)_2 \ldots\ldots \text{(1) Or}$$

$$2C_3S\ (Alite) + 6H \rightarrow (C - S - H) + 3CH(Portlandite)$$

$$2Ca_2SiO_4 + 4H_2O \rightarrow 3CaO.2SiO_2.3H_2O + Ca(OH)_2 \ldots\ldots \text{(2) Or}$$

$$2C_2S\ (Belite) + 4H \rightarrow (C - S - H) + CH(Portlandite)$$

$$Ca(OH)_2 + H_4SiO_4 \rightarrow Ca^{+2} + H_2SiO_4^{-2} + 2H_2O \rightarrow CaH_2SiO_4.2H_2O \ldots\ldots \text{(3) Or}$$

$$CH(Portlandite) + SH \rightarrow (C - S - H)$$

The aged CRCA has been exposed to concrete hydration components. The reaction of conversion of CH crystals that are accumulated on the CRCA surface to CSH particles is becoming a main source for producing CSH particles. This is achieved under pozzolanic action which transforms the amounts of CH crystals into CSH particles by the pozzolanic reaction (equation 3). The accumulated CSH particles fill the microcracks due to their small size compared with CH crystals resulting in microcrack improvement and ITZ densification.

As can be seen in Figure 2, there is an inverse relationship between the microcrack width and length, and increasing temperatures. The microcrack width and length are sharply decreased through heat treatment between (0-500°C). It is interesting to note that there is a slight increase, which can be negligible, to microcrack width at 500°C compared with heat treatment at 350°C. This means there is little impact of heat treatment type at high temperatures on microcrack width. However, heat treatment has a negative influence on other surface properties of aggregate and mortar as will be discussed later in this investigation. Therefore, the logarithmic equation with high regression obviously reflects strong correlation between heat treatment and microcrack width and length through this kind of treatment. From Table 3, the obtained results also revealed that acid treatment for both strong and weak acid is highly successful to lowering width and length of microcracks in the ITZ. However, treatment using weak acid seems to be more effective than strong acid due to a slight difference in obtained outcomes for both types of treatment compared with microcrack properties of untreated CRCA.

5.2 Elemental composition behavior on both sides of ITZ

Figures 9-a and 9-b present the atomic percentages of calcium (Ca), silicon (Si) and Ca/Si ratio from the outcomes of EDAX analysis (Appendix A), which was conducted on both sides of the ITZ; mortar side and aggregate side, were interpreted as a schematic diagram. The analysis of untreated CRCA revealed that there is a significant difference in Ca atoms between the mortar and the aggregate side indicating a higher percentage of CH particles on the mortar side that is mainly responsible for high porosity in the ITZ. From the obtained results of heat treatment at 250°C, it is concluded that a considerable decrease of Ca atoms with a high increase of Si atoms resulted in a significant enhancement for the ITZ for the mortar side as compared with the aggregate surface. It is notable that a reduction in the Ca/Si ratio is observed, indicating a significant transformation of the CSH phase which is substantially responsible for ITZ improvement.

The outcomes of acid treatments showed that HCl treatment seems to be more effective than acetic acid in terms of Ca atom behavior for both sides of aggregate and mortar indicating a high degree of transformation to CH crystals. Additionally, it is interesting to note that a high increase in Si atoms is registered through acetic acid treatment compared with HCl acid for the aggregate side, whereas HCl acid treatment is more effective for increasing Si atoms for the mortar side than acetic acid. This could be explained by two factors: firstly, there is a significant variance in the ability of strong and weak acids to attack the surface adhered mortar, and secondly, the surface material type. De Juan & Gutiérrez mentioned that HCl treatment cannot be used to treat RCA with limestone aggregates due to the adverse acid attacks on this type of aggregate. Moreover, the obtained results demonstrated that there is a considerable reduction of Ca/Si ratio for the aggregate side using acetic acid treatment as compared to HCl acid treatment, whereas HCl acid seems to be more successful for lowering the Ca/Si ratio on the mortar side, resulting in a significant transformation of CSH phase.

The atomic Ca/Si ratios on both sides of the ITZ measured by SEM coupled with EDAX are plotted in Figure 10. It is shown that a significant difference was observed in the behavior of atomic Ca/Si ratio between aggregate and the mortar side of the ITZ. For a temperature range between 20-350°C, the atomic Ca/Si ratio of the mortar side was sharply decreased, whereas it was registered that there is a slight decrease to the same ratio on the aggregate side of the ITZ. It is also demonstrated that heat treatment at higher temperatures between (350-500°C) has a negative influence on atomic Ca/Si ratio for both aggregate and the mortar side of the ITZ. However, the Ca/Si ratio on the mortar side is significantly affected by higher temperatures through increase of the Ca/Si ratio compared with the aggregate side which is only slightly influenced by the same conditions. The significant regression clearly indicates that the behavior of the atomic Ca/Si ratio on both sides of the ITZ and heat treatment are considerably related.

5.3 Intermix phases behavior on both sides of ITZ

Figure 11 represents the modification of intermix phases on both sides of the ITZ; aggregate and mortar side through different treatment types. Generally, it is thoroughly noticeable that the obtained results of the Ca/Si and the (Al + Fe)/Ca ratios reflect broad transformations of intermix phases on both sides of the ITZ. However, substantial improvement of transformation to CSH phase was registered for various treatment types. For untreated CRCA, the ratios of Ca/Si and (AL+Fe)/Ca indicate that the intermixed material on the surface of mortar and the aggregate side of the ITZ consists of different phases. As clearly shown, the position of the intermix phase is located in a transition area, which means, there is no certain predominant material among various phases for both surfaces of aggregate and mortar. Nevertheless, a significant difference was observed regarding the Ca/Si ratio which refers to the existence of a large variation between constituent materials of the two surfaces.

For heat treatment type, it is revealed that the best performance of transformation to CSH phase is recorded at 250°C recording Ca/Si ratio valued 2.5 for aggregate side of ITZ, whereas the mortar side enhancement through CSH transformation at 350°C exhibits as an optimum behavior with 2.46 of Ca/Si ratio. It is interesting to note that the Ca/Si ratio at 250°C was significantly lowered to 1.34 compared with the value at 350°C. This can be explained by the possibility of secondary ettringite formation due to a high percentage of (Al+Fe/Ca) (ratio 0.46). Erdem et al. supposed that the release of sulfate or a high amount of Al, Fe and S may promote ettringite recrystallization. Therefore, there is deviation from the CSH to AFM phase though lowering Ca/Si ratio. The obtained results of heat treatment at 500°C clearly present a negative impact of high temperature on transformation to the CH phase due to a considerable increase in Ca atoms compared with untreated CRCA for both sides of the ITZ; aggregate and mortar. It could be expected that material decomposition occurred at higher temperatures. Al-Bayati et. al (2016) mentioned that Thermal Gravimetric Analysis (TGA) provided more details about the mass loss and chemical breakdown of compounds such as H2O and CO2 due to exposure to different temperatures. TGA studies indicated that the mass loss between 105°C-200°C is related to vaporized water in pores and poorly hydrated C-S-H, whereas loss is correlated with water dissociation from well hydrated C-S-H between 200°C-420°C. $Ca(OH)_2$ decomposes between temperatures 420°C-550°C, whereas poor and well crystalline CaCO3 molecules dissociate to release CO2 between 550°C-720°C and 720°C-950°C, respectively. However, these temperature ranges are slightly different due to many factors such as aggregate type and chemical composition.

The outcomes of acid treatment indicated that there is a significant difference in CSH transformation between the aggregate and mortar sides of the ITZ for HCl acid treatment though approximate closer values Ca/Si ratios 1.84 and 1.17 respectively were recorded. The obtained results of acetic acid treatment revealed that there is a considerable difference between the aggregate and mortar side (0.88) and (2.32) resulting in significant phase transformation.

5.4 Influence of treatment types on surface properties

5.4.1 Pore size in mortar surface

Pore size behavior of CRCA is presented in Figure 12 and Table 4 based on the captured images of SEM test in Figures 13-18. The obtained outcomes of heat treatment clearly indicate that there is a dramatic decrease in pore size through a temperature range of (0-350°C). By contrast, the pore size is sharply increased within a temperature range of (350-500°C), resulting in a considerable negative effect of higher temperatures on pore size of the mortar surface. More specifically, it is highly interesting to note that the pore size through heat treatment at 500°C is increased three times compared with pore size of untreated CRCA. The obtained results also demonstrated that a successful acid treatment is registered for both types; strong and weak acid for decreasing pore size of CRCA. However, the treatment using strong acid seems to be more successful based on the laboratory results.

5.4.2 Width and length of matrix cracks

Properties of matrix cracks including width and length, and behavior of cracks on mortar surface of CRCA for various treatment types, are demonstrated in Figures 19-a, 19-b and Table 5. Whereas, the SEM images of matrix cracks are given in Figures 20-25. It is shown that there is a negative influence of heat treatment on properties of matrix cracks; width and length on the mortar surface. The width and length of matrix cracks are gradually increased within the temperature range of (0-350°C), whereas the properties of cracks, width and length, are sharply increased through rising temperatures to 500°C resulting in a considerable impact for heat treatment at higher temperatures. The obtained outcomes also revealed that the behavior of both properties exhibit as a polynomial equation and strongly correlate with heat treatment due to high regression. Table 5 displays properties of matrix cracks including width and length using acid treatment. The obtained results indicated that there is a negative effect for both types of acid treatment on properties of matrix cracks through increasing width and length compared with the same properties of matrix cracks for untreated CRCA. It is concluded that the influence of both acid treatments is similar to impact of heat treatment within temperature range (0-350°C).

5.4.3 Matrix (macro) cracks density

The obtained results of crack density and the relationship between crack density and properties of matrix cracks including width and length are presented in Figures 26-27. The outcomes demonstrate that crack density is slightly raised in a temperature range of (0-350°C), whereas crack density is dramatically increased at a higher temperature range of (350-500°C). However, the overall behavior shows a strong correlation between the crack density and heat treatment.

The outcomes also demonstrate that properties of matrix cracks including width and length are significantly correlated with crack density. As crack density increases, both matrix crack properties, width and length, are increased. However, a significant difference in behavior is noticeable between the two properties. The developed relationship from regression analysis between the crack density and the width of matrix cracks presents itself as a polynomial equation, and this exponential equation completely describes the relationship between crack density and length of matrix cracks.

Conclusions

The influence of different treatment types on ITZ properties, especially microcracks and mortar surface properties, have been investigated in this study. Based on the experimental results, the following conclusions could be drawn:

- Heat treatment method is highly successful in improving properties of microcracks in the ITZ including width and length of microcracks. It is concluded that there is an inverse relationship between microcrack properties including width and length, and increasing temperatures. However, heat treatment at high temperature (500°C) has very little influence on microcrack width due to a slight increase compared with microcrack width at 350°C.
- Acid treatment is an effective technique for lowering width and length of microcracks in the ITZ. However, treatment using weak acid appears to be more successful than strong acid due to a slight difference in the obtained results for both types of acid treatment.
- Heat treatment at 250°C exhibits the best performance by considerably decreasing the Ca atoms with highly increasing the Si atoms for the mortar side compared with the aggregate surface resulting in a considerable decrease in the Ca/Si ratio which indicates significant enhancement for the ITZ zone. However, there is a negative impact for heat treatment at higher temperatures between (350-500°C) on the atomic Ca/Si ratio for both aggregate and the mortar side of the ITZ.
- Utilization of acetic acid treatment leads to a significant reduction of the Ca/Si ratio for the aggregate side compared with HCl acid treatment, whereas HCl treatment seems to be more successful for lowering the Ca/Si ratio on the mortar side.

- Best performance of transformation to the CSH phase was observed at 250°C for the aggregate side of the ITZ, whereas the mortar side improvement through CSH transformation is recorded at 350°C as an optimum behavior. It is concluded that the use of acetic acid treatment is more successful for CSH transformation for the mortar side of the ITZ. Whereas, HCl acid treatment seems to be highly effective for CSH transformation on the aggregate side of the ITZ.
- Heat treatment at temperatures ranging between (0-350°C) has a strong positive influence on pore size reduction due to dramatic decrease of pore volume values. Whereas, there is a significant negative impact of heat treatment within a temperature range of (350-500°C) due to considerable increase of pore size compared with untreated CRCA. A successful acid treatment is recorded for both types: strong and weak acid for decreasing pore size of CRCA. However, the treatment method using strong acid seems to be more effective due to a slight difference compared with weak acid.
- Heat treatment has a negative effect on the properties of the matrix cracks including width and length on the mortar surface. This influence is considerably increased at temperatures that ranged between (350-500°C). It is concluded that the impact of both acid treatments on properties of matrix cracks including width and length is similar to the influence of heat treatment at temperatures between (0-350°C).
- Crack density on the mortar side is strongly correlated with properties of matrix cracks including width and length due to a significant regression. However, a considerable difference in the behavior is clearly observed between properties of matrix cracks and crack density.

Acknowledgement

The authors gratefully acknowledge the funding provided by Ministry of Higher Education and Scientific Research/Iraq through Iraqi Scholarship/Doctoral Program. The authors are also grateful to Steed and Evans Ltd in the Region of Waterloo, Ontario for providing Recycled Concrete Aggregate material. A special thanks to Dr. Nafiseh Moghimi in the Waterloo Advanced Technology Laboratory (WATLab)/University of Waterloo for her substantial support throughout the Interface Transition Zone (ITZ) tests. Her effort, advice and patience in characterizing this region are greatly appreciated.

References

Akçaoğlu, T., Tokyay, M., & Çelik, T. 2005. "Assessing the ITZ microcracking via scanning electron microscope and its effect on the failure behavior of concrete". *Cement and Concrete Research*. 35(2): 358-363.

Al-Bayati, H. K. A., Das, P. K., Tighe, S. L., & Baaj, H. 2016. "Evaluation of various treatment methods for enhancing the physical and morphological properties of coarse recycled concrete aggregate". *Construction and Building Materials.* 112: 284-298.

Cement Chemical Composition and Hydration. [Viewed 11 January 2016.] http://elearning.vtu.ac.in/16/ENotes/ConcreteTechnology/Unit1-RVR/Unit1-L2-RVR.pdf

Cwirzen, A., & Penttala, V. 2005. "Aggregate–cement paste transition zone properties affecting the salt–frost damage of high-performance concretes". *Cement and Concrete Research.* 35(4): 671-679.

Demie, S., Nuruddin, M. F., & Shafiq, N. 2013. "Effects of micro-structure characteristics of interfacial transition zone on the compressive strength of self-compacting geopolymer concrete". *Construction and Building Materials*. 41: 91-98.

Duan, P., Shui, Z., Chen, W., & Shen, C. 2013. "Effects of metakaolin, silica fume and slag on pore structure, interfacial transition zone and compressive strength of concrete". *Construction and Building Materials.* 44: 1-6.

Erdem, S., Dawson, A. R., & Thom, N. H. 2012. “Impact load-induced micro-structural damage and micro-structure associated mechanical response of concrete made with different surface roughness and porosity aggregates”. *Cement and Concrete Research.* 42(2): 291-305.
Erdem, S., Dawson, A. R., & Thom, N. H. 2012. “Influence of the micro- and nanoscale local mechanical properties of the interfacial transition zone on impact behavior of concrete made with different aggregates”. *Cement and Concrete Research*. 42(2): 447-458.
Gao, Y., De Schutter, G., Ye, G., Tan, Z., & Wu, K. 2014. “The ITZ microstructure, thickness and porosity in blended cementitious composite: Effects of curing age, water to binder ratio and aggregate content”. *Composites Part B: Engineering.* 60: 1-13.
Güneyisi, E., Gesoğlu, M., Algın, Z., & Yazıcı, H. 2014. “Effect of surface treatment methods on the properties of self-compacting concrete with recycled aggregates”. *Construction and Building Materials.* 64: 172-183.
Jawahar, J. G., Sashidhar, C., Reddy, I. R., & Peter, J. A. 2013. “Micro and macro level properties of fly ash blended self-compacting concrete”. *Materials & Design.* 46: 696-705.
Kong, D., Lei, T., Zheng, J., Ma, C., Jiang, J., & Jiang, J. 2010. “Effect and mechanism of surface-coating pozzalanics materials around aggregate on properties and ITZ microstructure of recycled aggregate concrete”. *Construction and Building Materials.* 24(5): 701-708.
Leemann, A., Münch, B., Gasser, P., & Holzer, L. 2006. “Influence of compaction on the interfacial transition zone and the permeability of concrete”. *Cement and Concrete Research.* 36(8): 1425-1433.
Li, J., Xiao, H., & Zhou, Y. 2009. “Influence of coating recycled aggregate surface with pozzolanic powder on properties of recycled aggregate concrete”. *Construction and Building Materials*. 23(3): 1287-1291.
Li, W., Xiao, J., Sun, Z., Kawashima, S., & Shah, S. P. 2012. “Interfacial transition zones in recycled aggregate concrete with different mixing approaches”. *Construction and Building Materials.* 35: 1045-1055.
Ministry of Natural Resources (MNR.). *State of the Aggregate Resource in Ontario Study: Ontario Ministry of Natural Resources*. February 2010. [Viewed 4 March 2016.] http://www.mnr.gov.on.ca/stdprodconsume/groups/lr/@mnr/@aggregates/documents/document/286996.pdf
Mukharjee, B. B., & Barai, S. V. 2014. “Influence of incorporation of nano-silica and recycled aggregates on compressive strength and microstructure of concrete”. *Construction and Building Materials.* 71: 570-578.
Ontario Provincial Standard Specifications (OPSS.MUNI 1010). *Material Specification for Aggregates – Base, Subbase, Select Subgrade, and Backfill Material: Ontario Ministry of Transportation, Ontario, Canada.* November 2013.
Otsuki, N., Miyazato, Shin-ichi, Yodsudjai, W. 2003. “Influence of Recycled Aggregate on Interfacial Transition Zone, Strength, Chloride Penetration and Carbonation of Concrete”. *Journal of Materials in Civil Engineering.* 15 (5): 443-451.
Poon, C. S., Qiao, X. C., & Chan, D. 2006. “The cause and influence of self-cementing properties of fine recycled concrete aggregates on the properties of unbound sub-base”. *Waste management*. 26(10): 1166-1172.
Poon, C. S., Shui, Z. H., & Lam, L. 2004. “Effect of microstructure of ITZ on compressive strength of concrete prepared with recycled aggregates”. *Construction and Building Materials.* 18(6): 461-468.
Purushothaman, R., Amirthavalli, R. R., & Karan, L. 2014. “Influence of treatment methods on the strength and performance characteristics of recycled aggregate concrete”. *Journal of Materials in Civil Engineering*. 27(5): 04014168.
Sun, X., Zhang, B., Dai, Q., & Yu, X. 2015. “Investigation of internal curing effects on microstructure and permeability of interface transition zones in cement mortar with SEM imaging,

transport simulation and hydration modeling techniques". *Construction and Building Materials*. 76: 366-379.
Tam, V. W., & Tam, C. M. 2008. "Diversifying two-stage mixing approach (TSMA) for recycled aggregate concrete: TSMA s and TSMA sc". *Construction and Building Materials*. 22(10): 2068-2077.
Tam, V. W., Gao, X. F., & Tam, C. M. 2005. "Microstructural analysis of recycled aggregate concrete produced from two-stage mixing approach". *Cement and Concrete Research*. *35*(6): 1195-1203.
Tam, V. W., Tam, C. M., & Le, K. N. 2007. "Removal of cement mortar remains from recycled aggregate using pre-soaking approaches". *Resources, Conservation and Recycling*. 50(1): 82-101.
Tragardh, J. 1999. "Microstructural features and related properties of self-compacting concrete. In Self-Compacting Concrete". In *1999 Proceedings of the First International RILEM Symposium.* Stockholm, Sweden.
Wang, X. H., Jacobsen, S., He, J. Y., Zhang, Z. L., Lee, S. F., & Lein, H. L. 2009. "Application of nanoindentation testing to study of the interfacial transition zone in steel fiber reinforced mortar". *Cement and Concrete Research*. 39(8): 701-715.
Wong, H. S., Zobel, M., Buenfeld, N. R., & Zimmerman, R. W. 2009. "Influence of the interfacial transition zone and microcracking on the diffusivity, permeability and sorptivity of cement-based materials after drying". *Mag. Concr. Res*. 61(8): 571-589.
Wu, K., Shi, H., Xu, L., Ye, G., & De Schutter, G. 2016. "Microstructural characterization of ITZ in blended cement concretes and its relation to transport properties". *Cement and Concrete Research*. 79: 243-256.
Xuan, D. X., Shui, Z. H., & Wu, S. P. 2009. "Influence of silica fume on the interfacial bond between aggregate and matrix in near-surface layer of concrete". *Construction and Building Materials*. 23(7): 2631-2635.
Zhang, J., Shi, C., Li, Y., Pan, X., Poon, C. S., & Xie, Z. 2015. "Performance enhancement of recycled concrete aggregates through carbonation". *Journal of Materials in Civil Engineering*. 27(11): 04015029.

Table 1: Physical properties of CRCA

CRCA	Specific Gravity ASTM C 127	Absorption, % ASTM C 127	Adhered Mortar, %		Micro-Deval Abrasion Loss, %ASTMD6928	Fractured Particles,% ASTM D5821	Aggregate Crushing Value BS 812-110	Flat & Elongated,% LS-608
			With steel ball	Without steel ball				
	2.421	3.74	2.53	1.08	16.03	95.72	23.28	0.44

Table 2. Microcrack width and length in ITZ zone before and after acid treatments

CRCA Treatment/ Property	Microcrack width (μm)	Microcrack length (μm)
CRCA untreated	129.70	780
CRCA soaking in HCl	5.29	209.1
CRCA soaking in C2H4O2	1.93	28.8

Table 3. Pore size in mortar surface before and after acid treatments

CRCA Treatment/ Property	Pore size (μm)
CRCA untreated	208.9
CRCA soaking in HCl	139.9
CRCA soaking in C2H4O2	156.1

Table 4. Matrix crack width and length on mortar surface before and after acid treatments

CRCA Treatment/ Property	Macro crack width (μm)	Macro crack length (μm)
CRCA untreated	0.70	20
CRCA soaking in HCl	2.68	35
CRCA soaking in C2H4O2	4.54	123

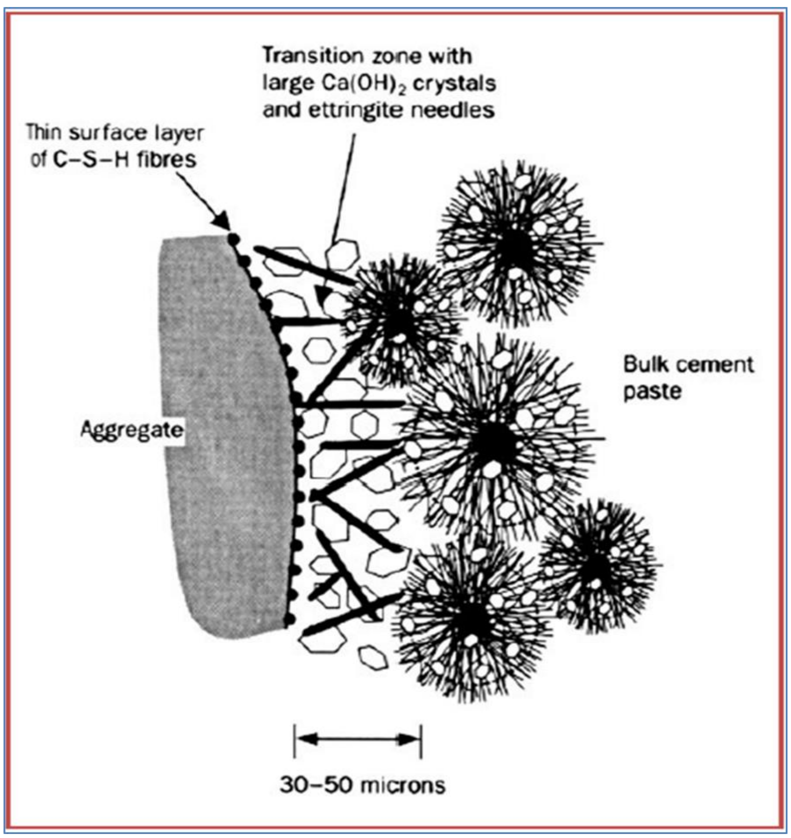

Figure 1: Schematic diagram of ITZ zone (Cement Chemical Composition and Hydration

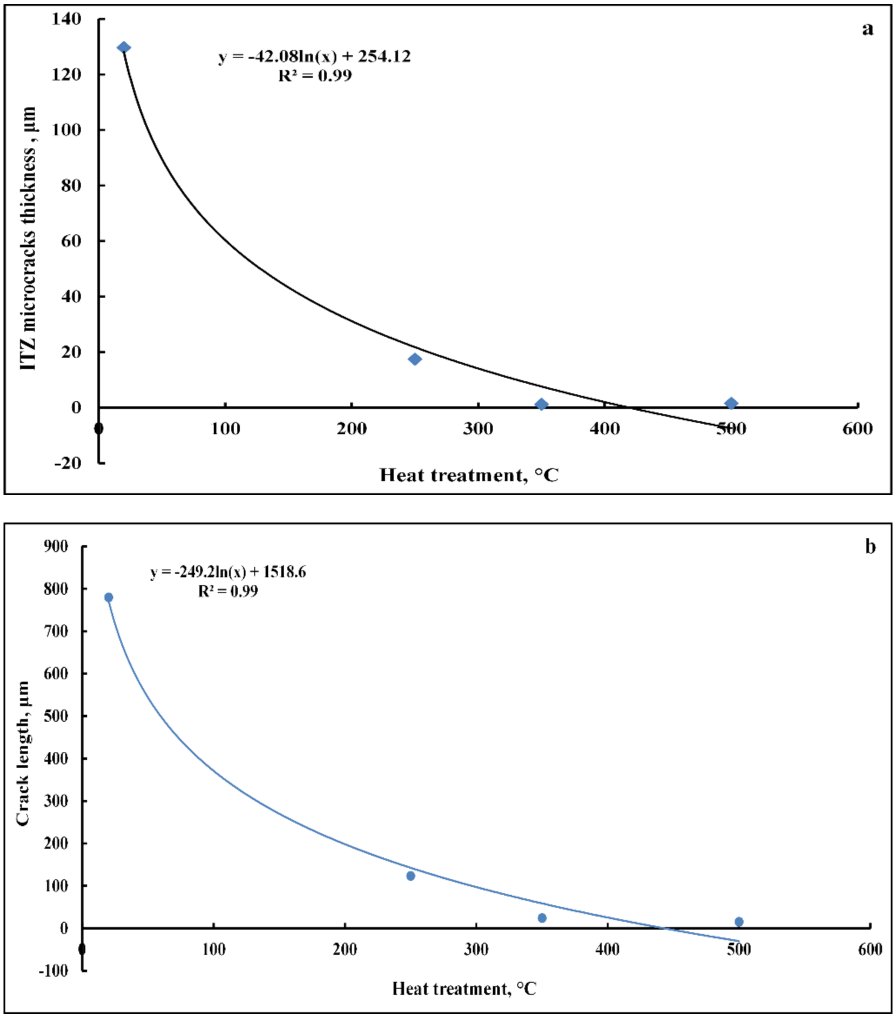

Figure 2: Behavior of ITZ microcrack through heat treatment:- a: width b: length

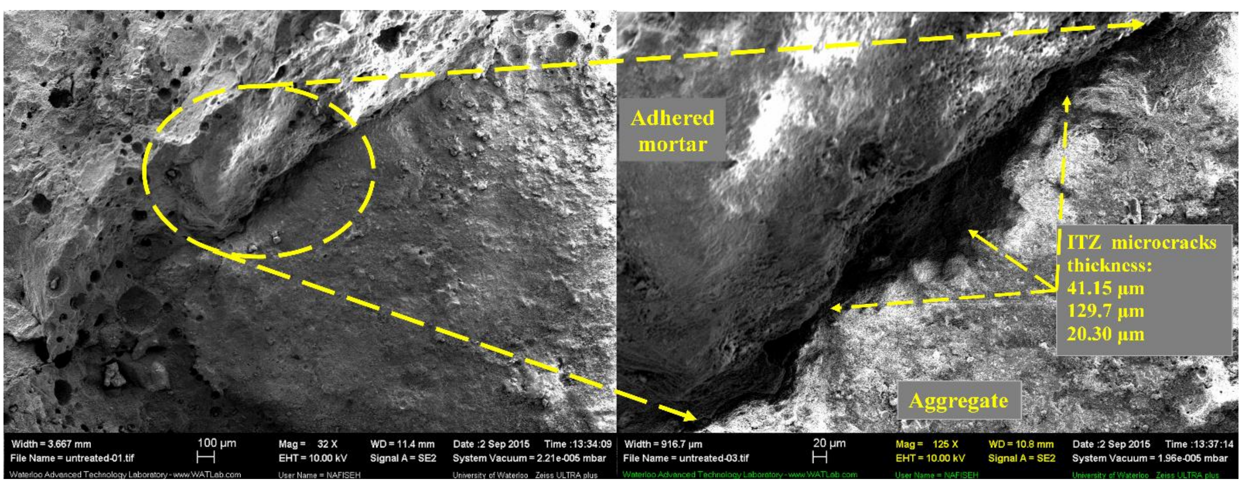

Figure 3: ITZ microcrack width to untreated CRCA

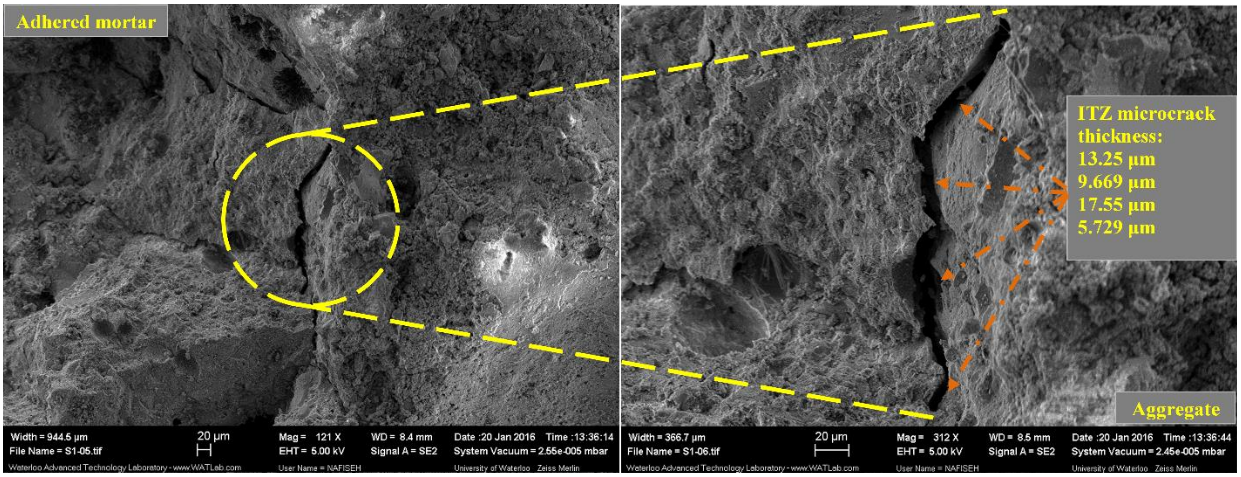

Figure 4: ITZ microcrack width to CRCA through heat treatment at 250°C

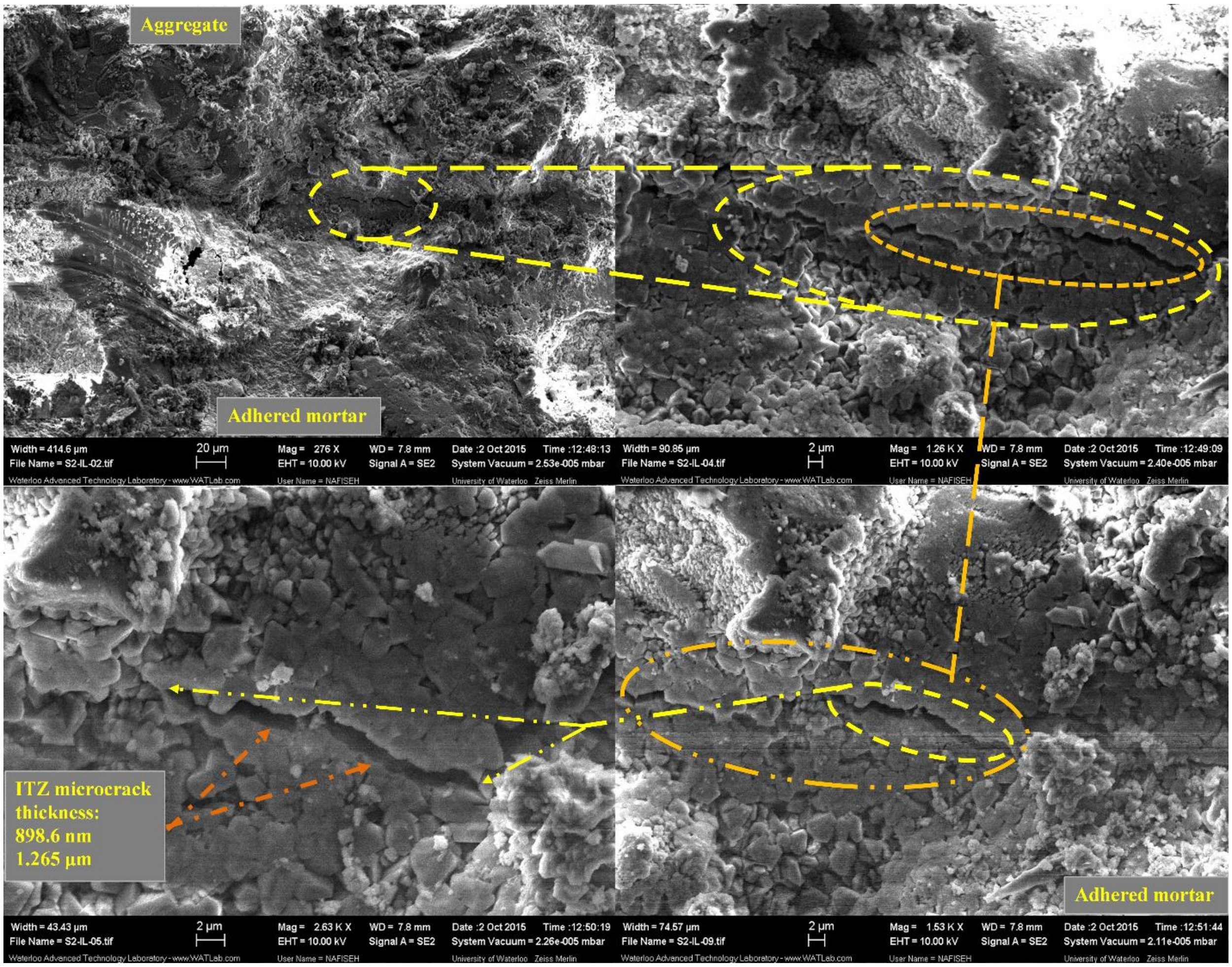

Figure 5: ITZ microcrack width to CRCA through heat treatment at 350°C

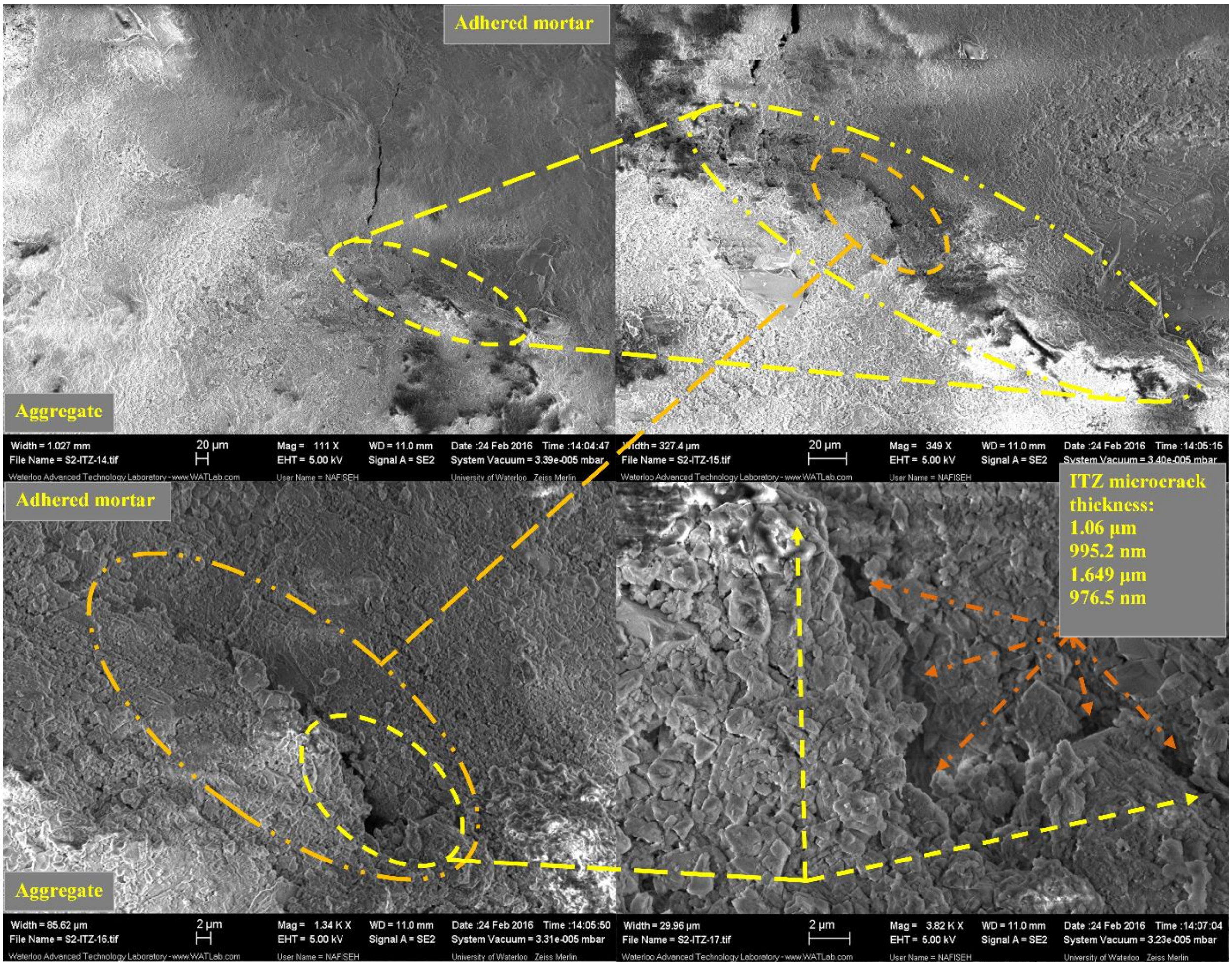

Figure 6: ITZ microcrack width to CRCA through heat treatment at 500°C

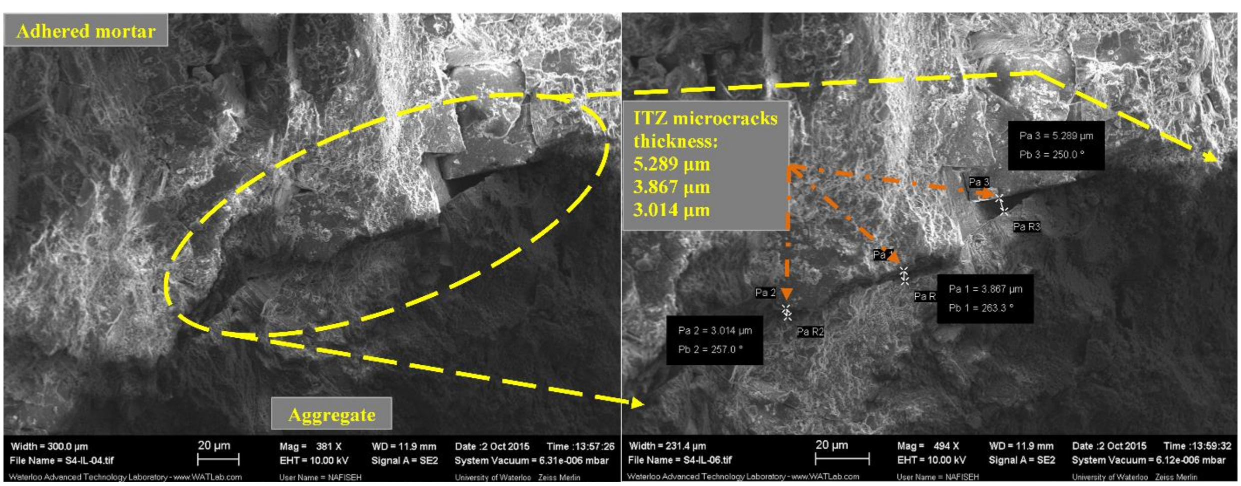

Figure 7: ITZ microcrack width to CRCA through acidic treatment with HCl

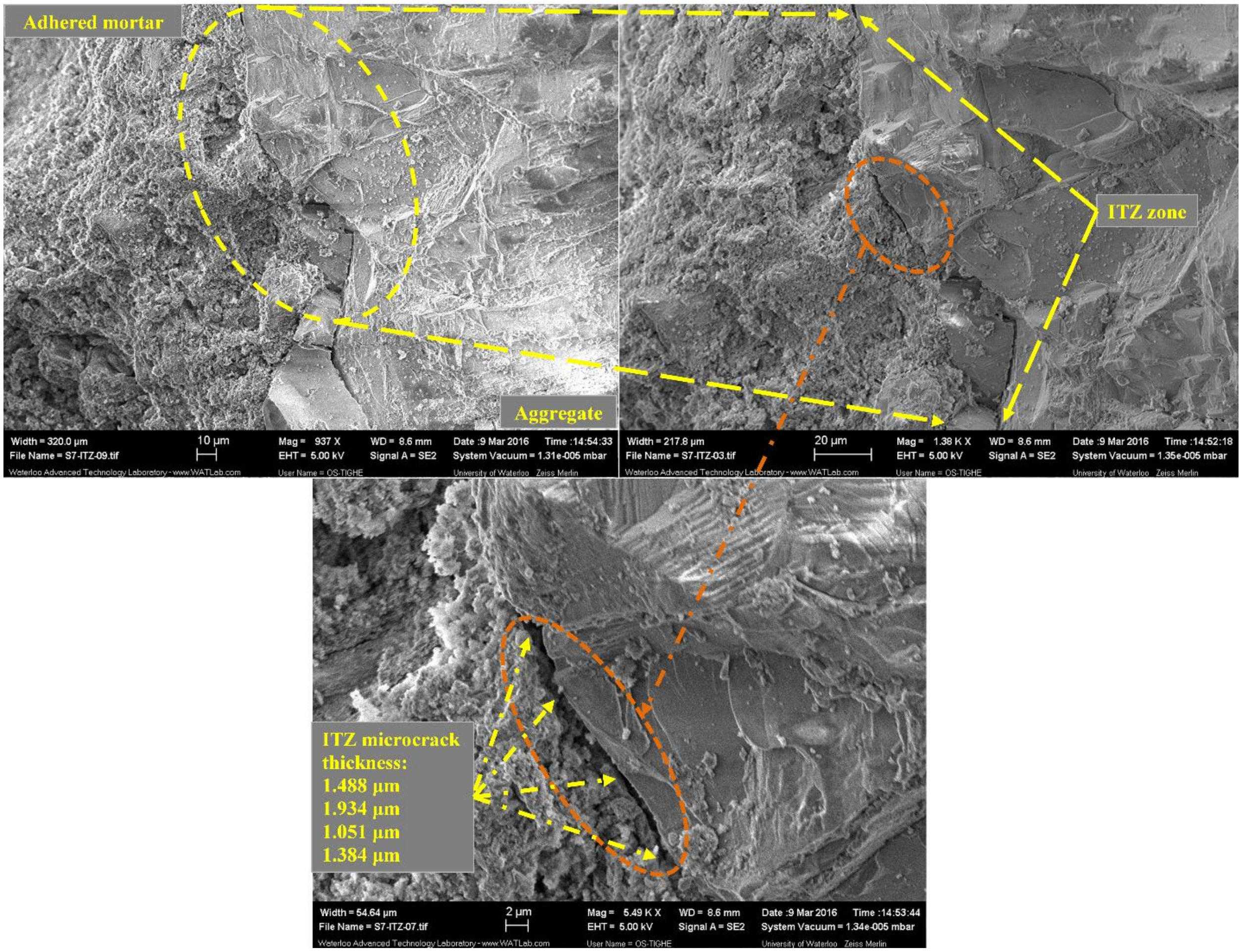

Figure 8: ITZ microcrack width to CRCA through acidic treatment with $C_2H_4O_2$

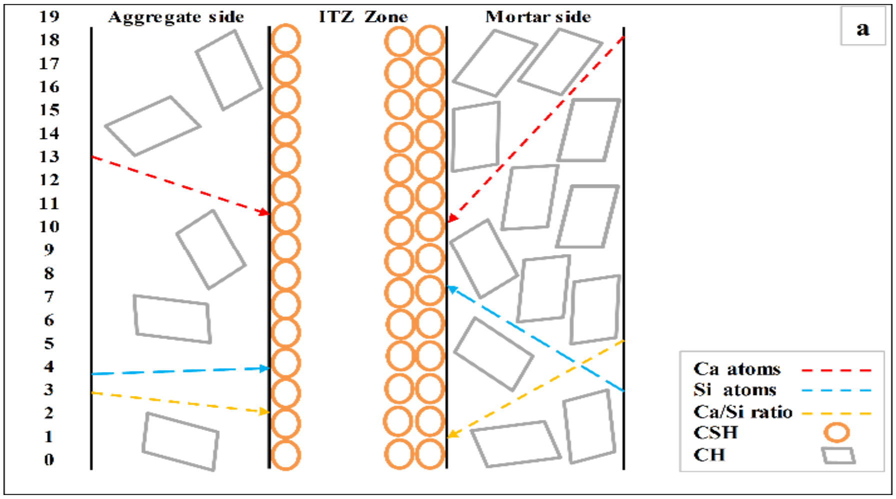

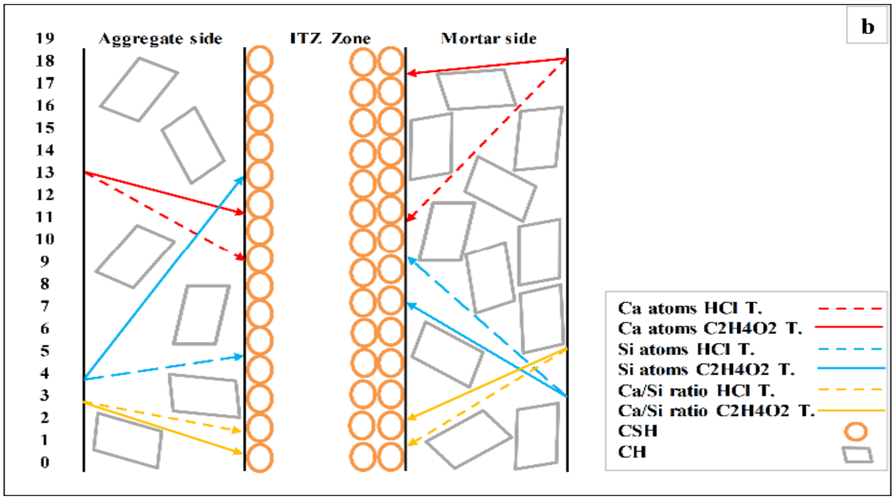

Figure 9: Schematic diagram of ITZ zone:- a: heat treatment at 250°C, b: acid treatments

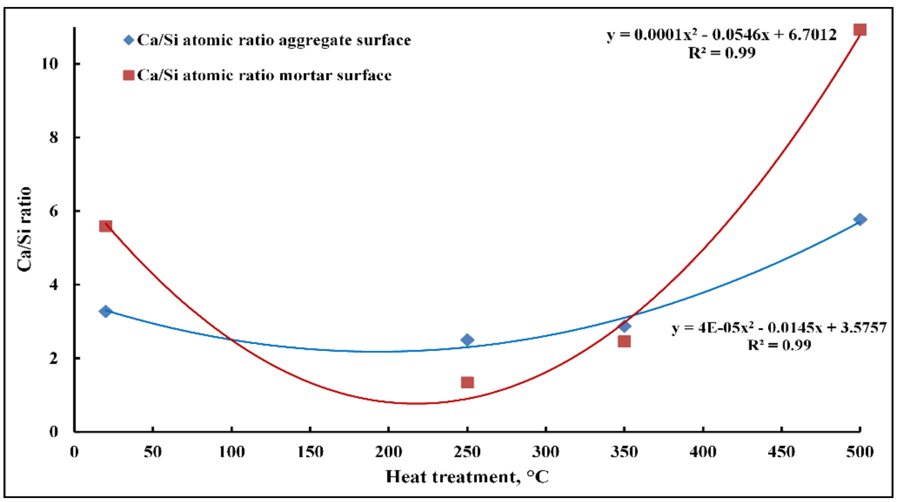

Figure 10: Ca/Si atomic ratio for aggregate and mortar surface through heat treatment

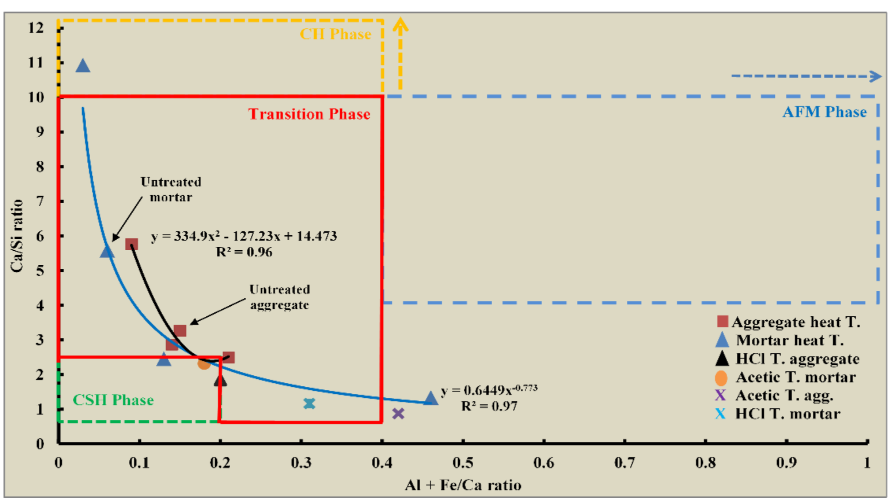

Figure 11: Intermix phases to mortar and aggregate of CRCA through heat treatment

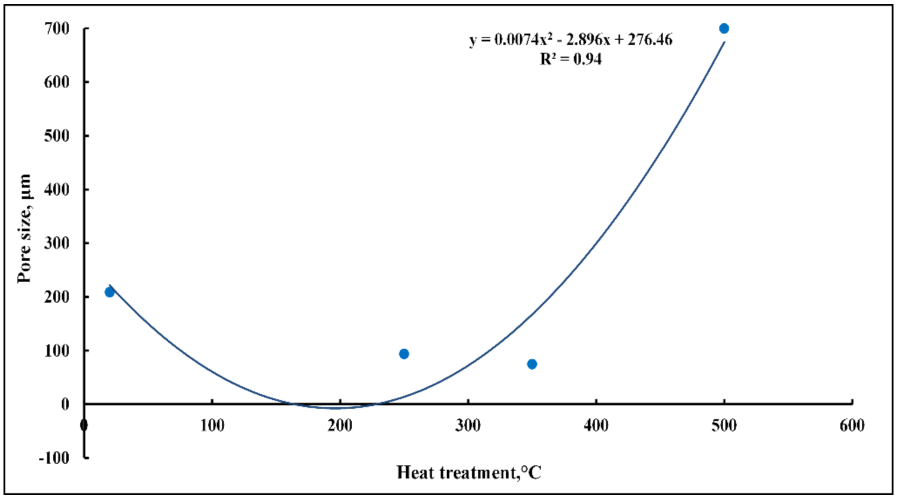

Figure 12: Pore size behavior through heat treatment

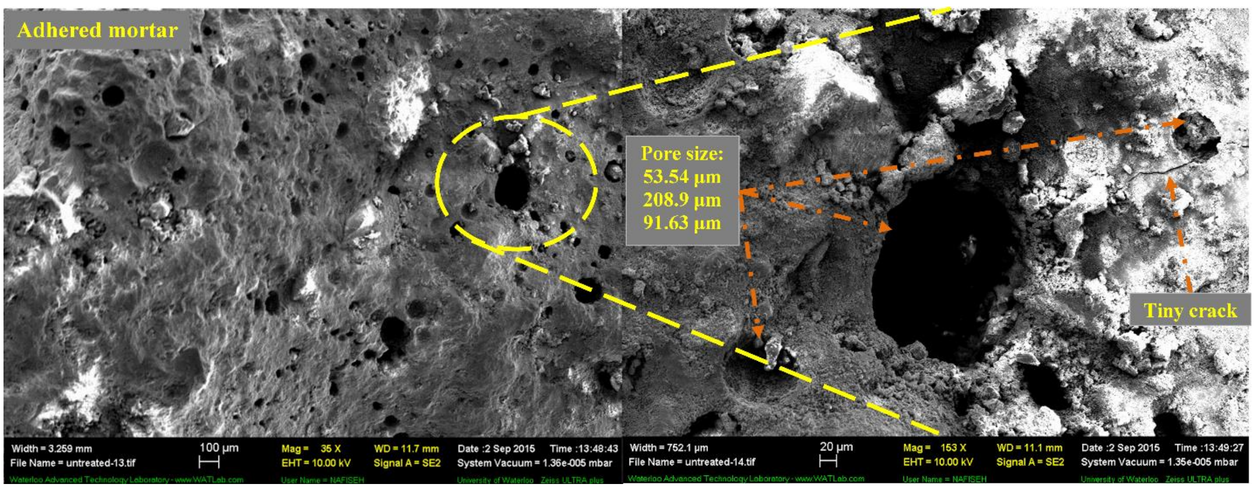

Figure 13: Pore size of mortar surface to untreated CRCA

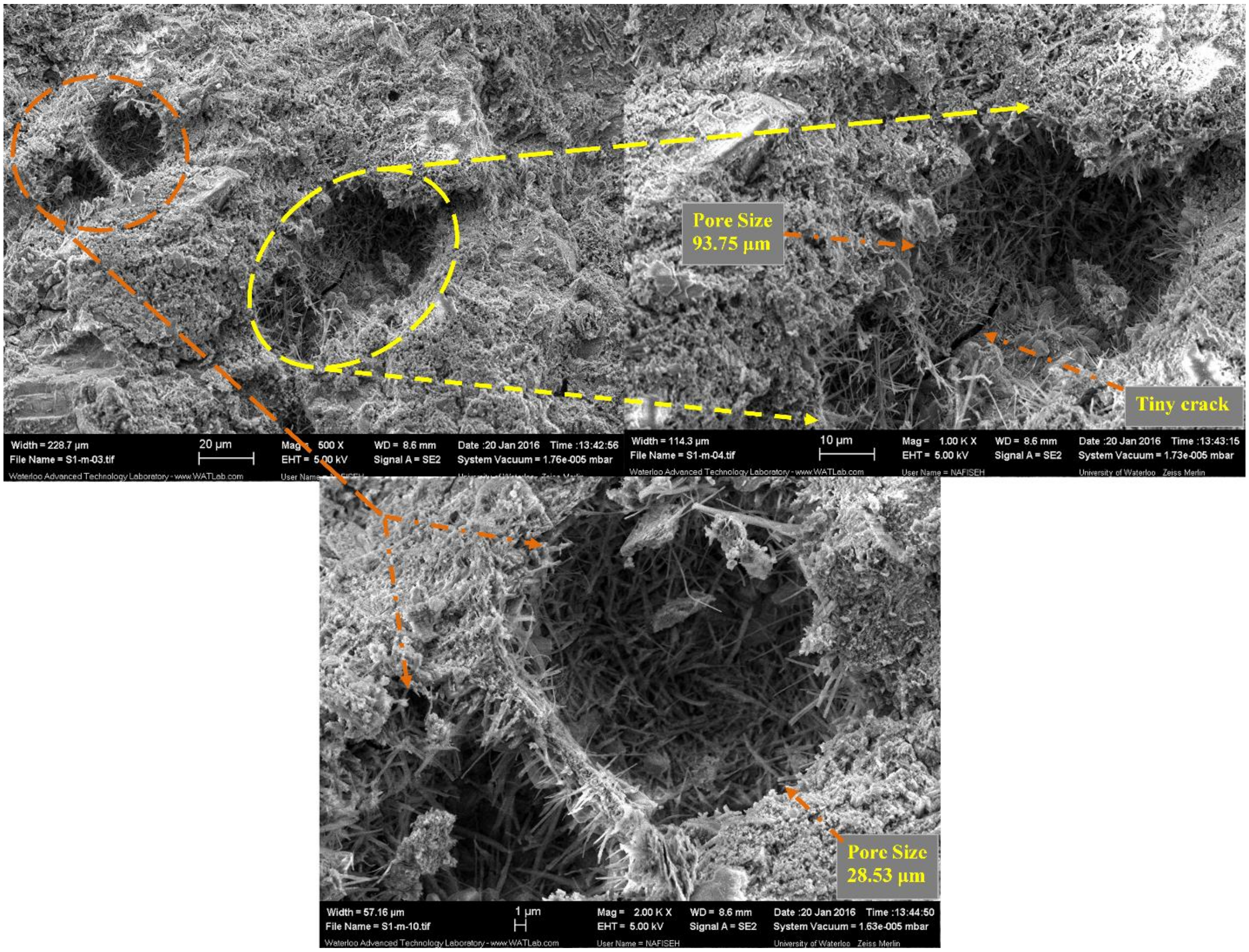

Figure 14: Pore size of mortar surface to CRCA through heat treatment at 250°C

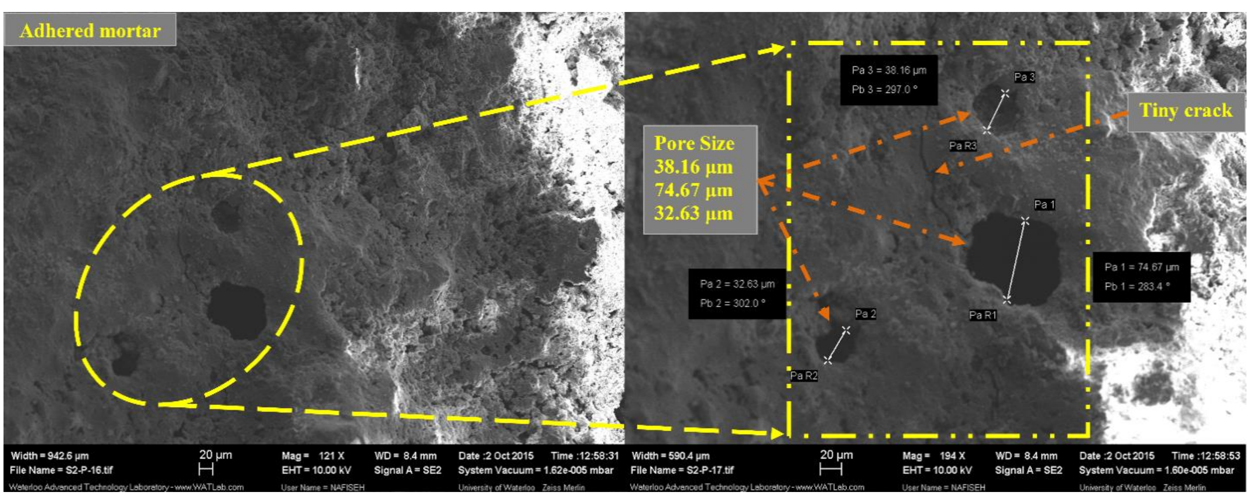

Figure 15: Pore size of mortar surface to CRCA through heat treatment at 350°C

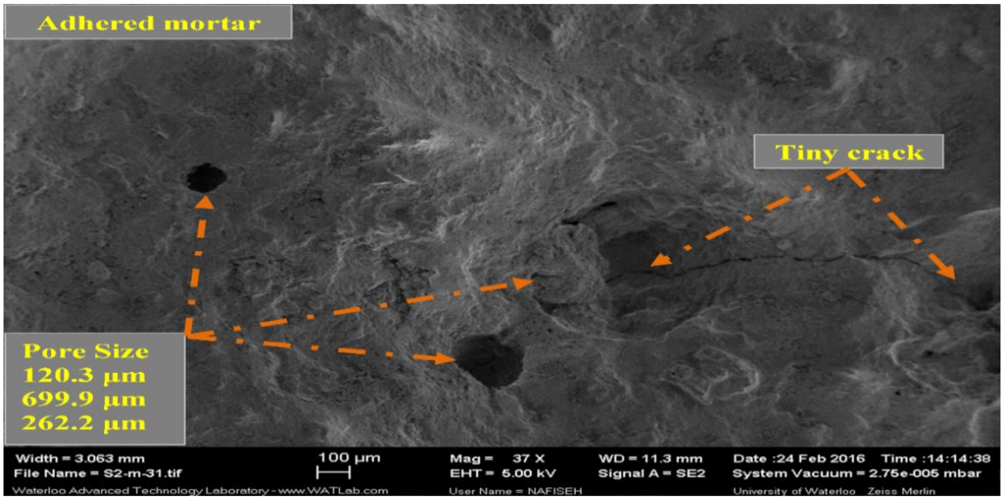

Figure 16: Pore size of mortar surface to CRCA through heat treatment at 500°C

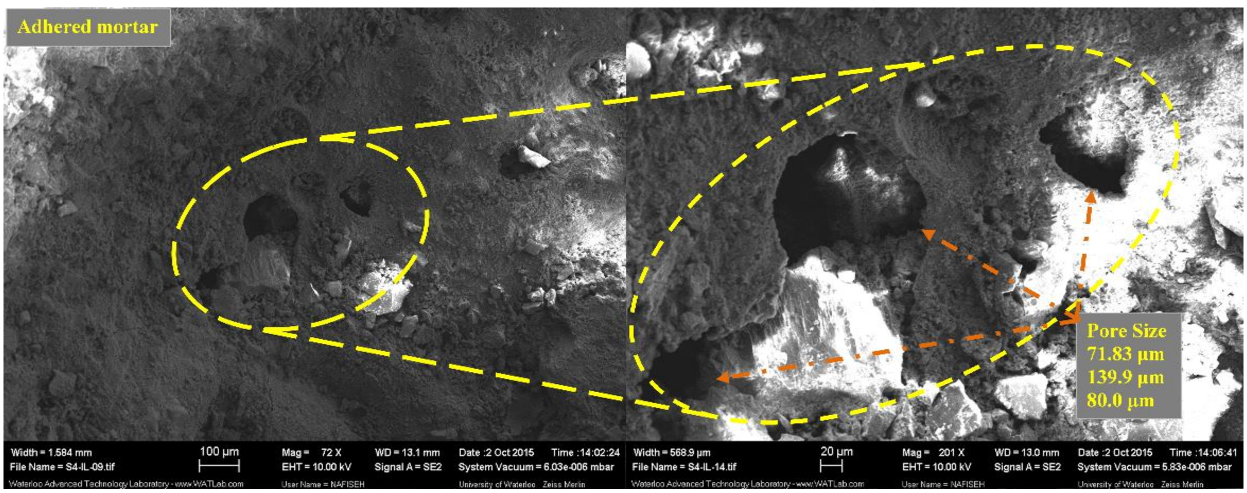

Figure 17: Pore size of mortar surface to CRCA through HCl treatment

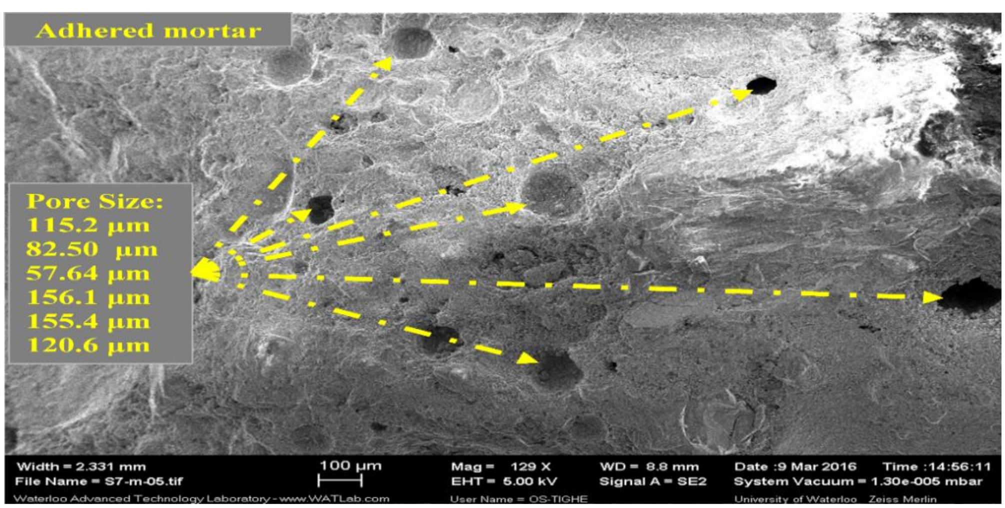

Figure 18: Pore size of mortar surface to CRCA through $C_2H_4O_2$ treatment

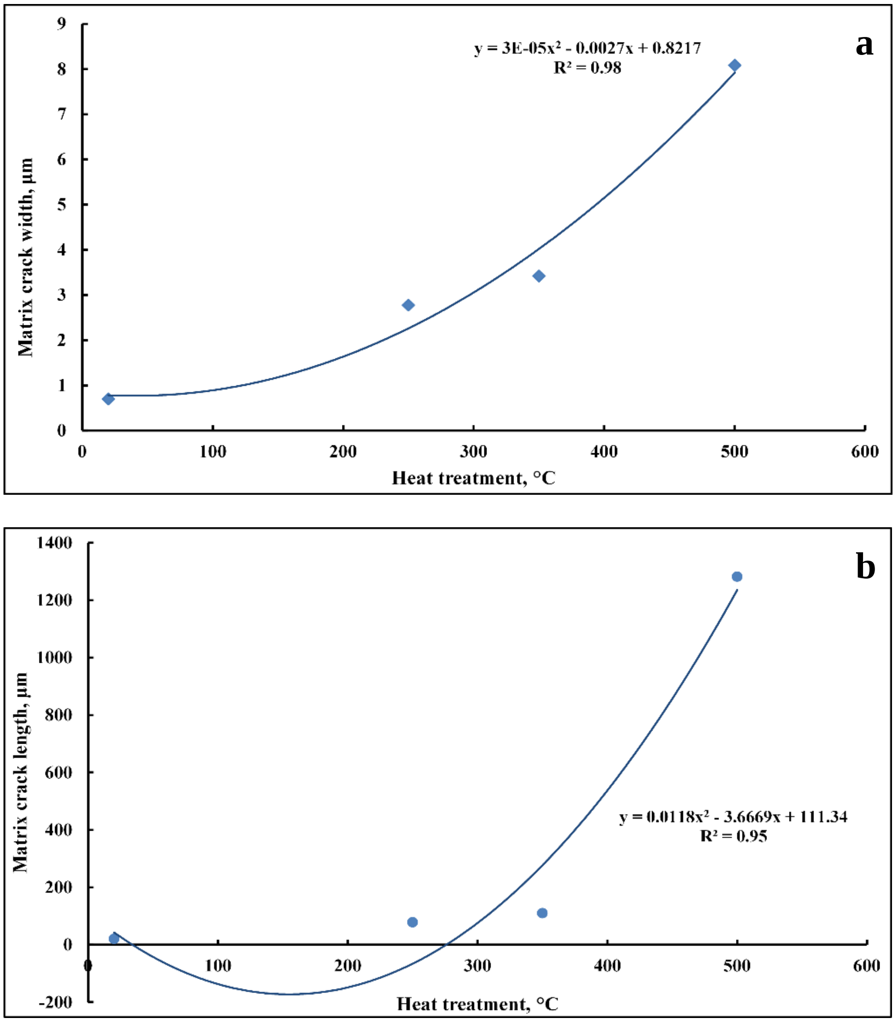

Figures. 19: Behavior of matrix cracks properties through heat treatment:- a: width, b: length

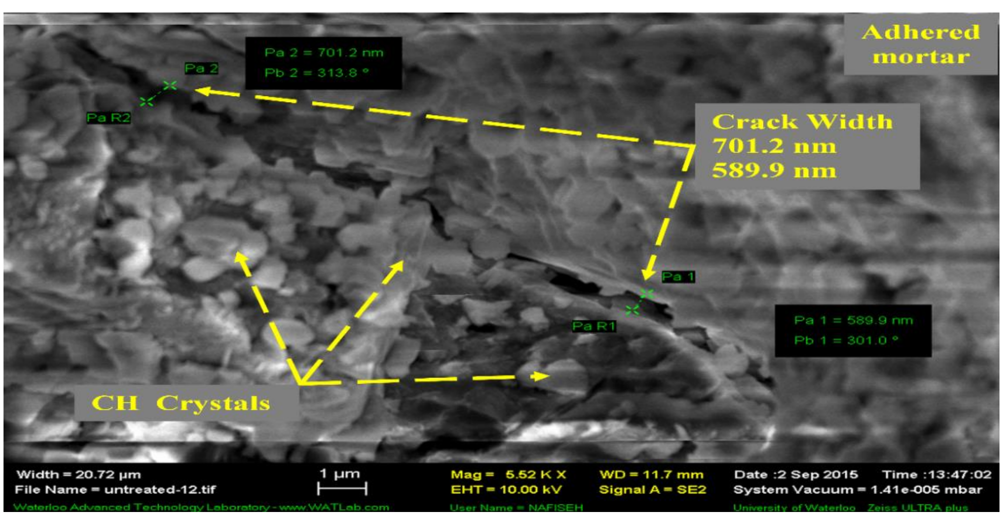

Figure 20: Matrix cracks on mortar surface to untreated CRCA

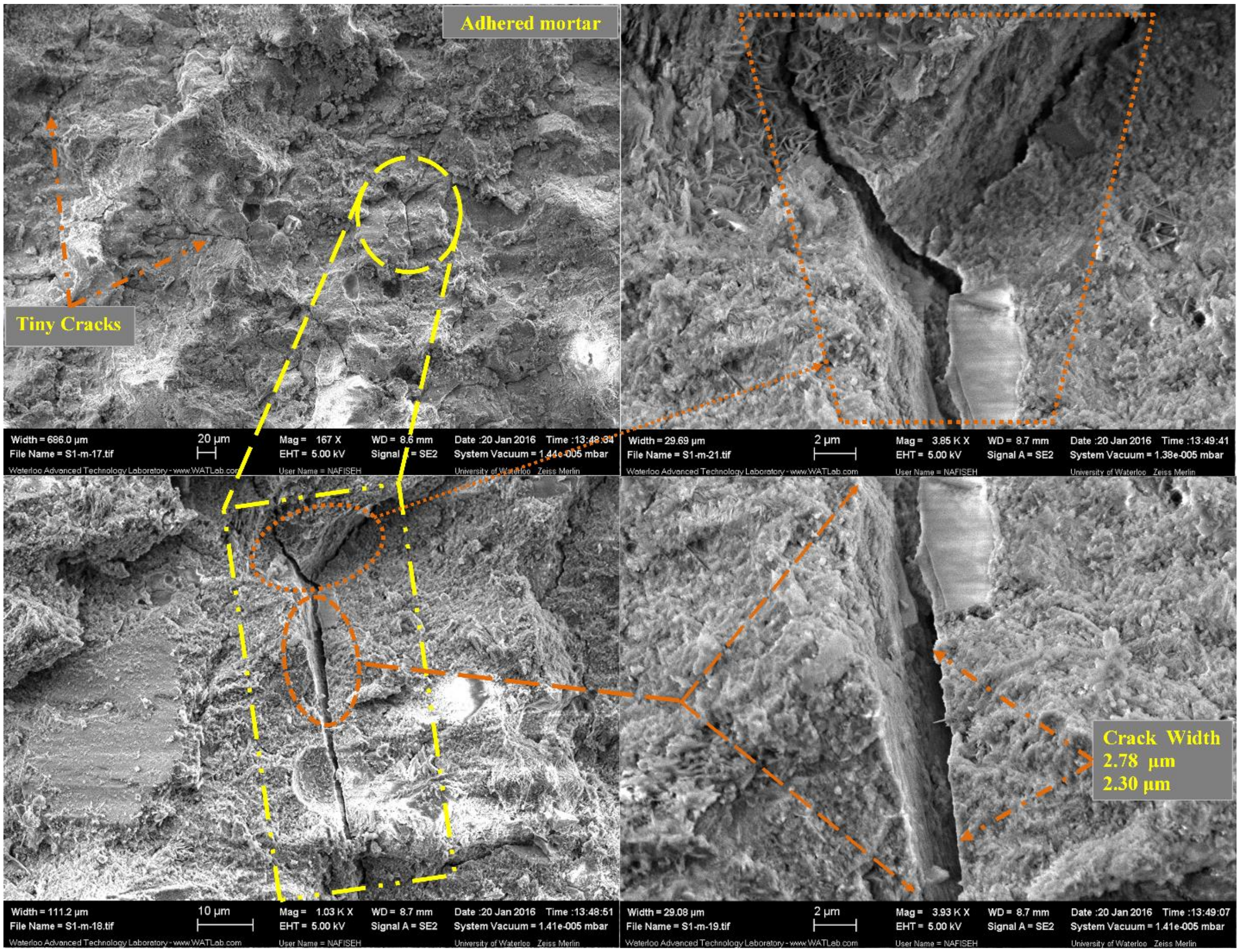

Fig. 21: Matrix cracks on mortar surface through heat treatment at 250°C

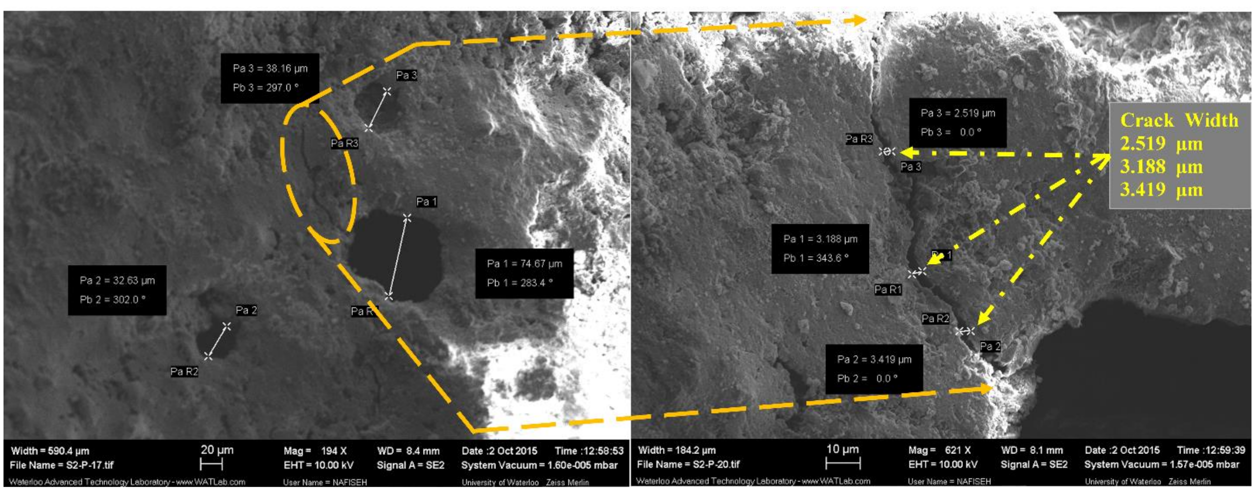

Figure 22: Matrix cracks on mortar surface through heat treatment at 350°C

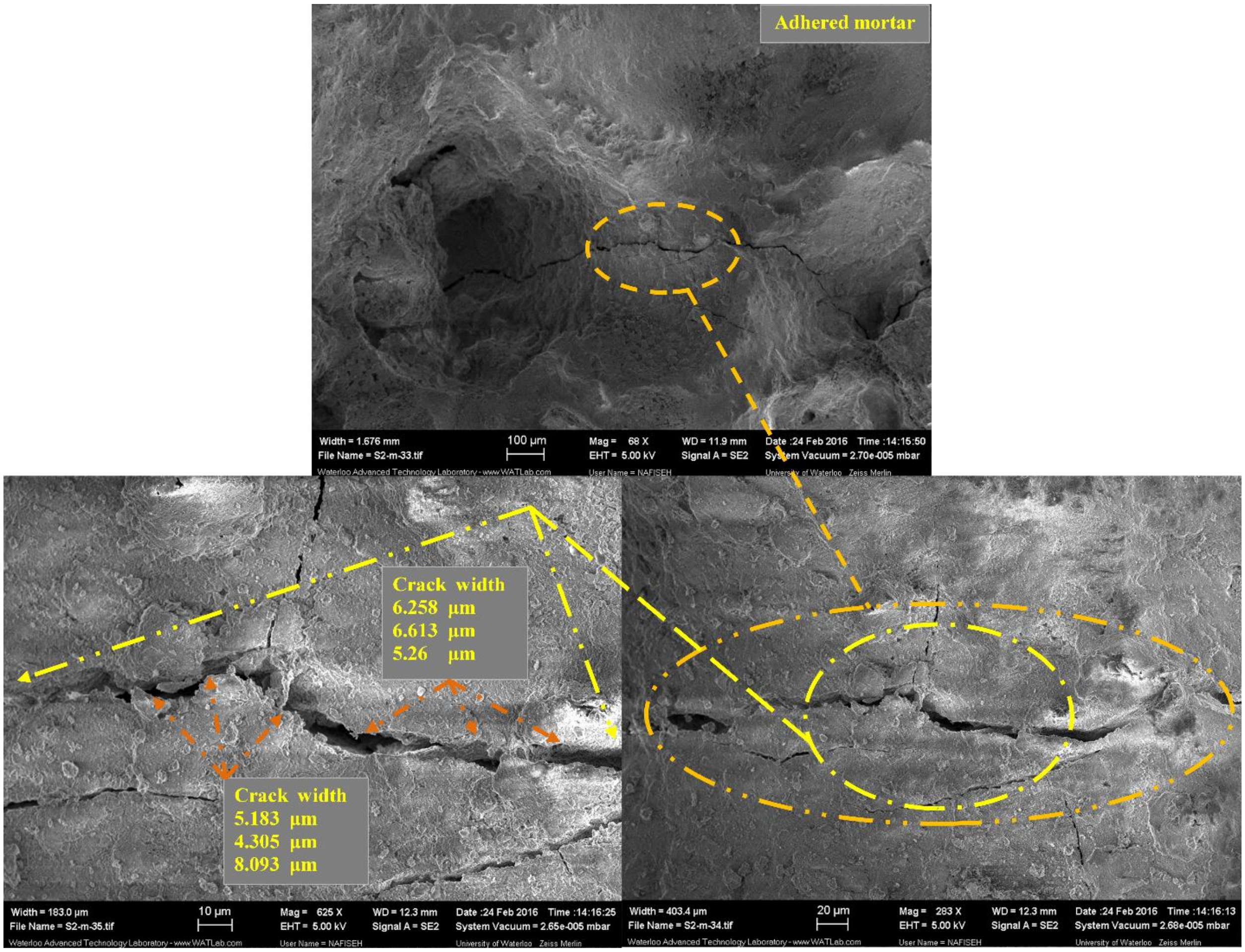

Figure 23: Matrix cracks on mortar surface through heat treatment at 500°C

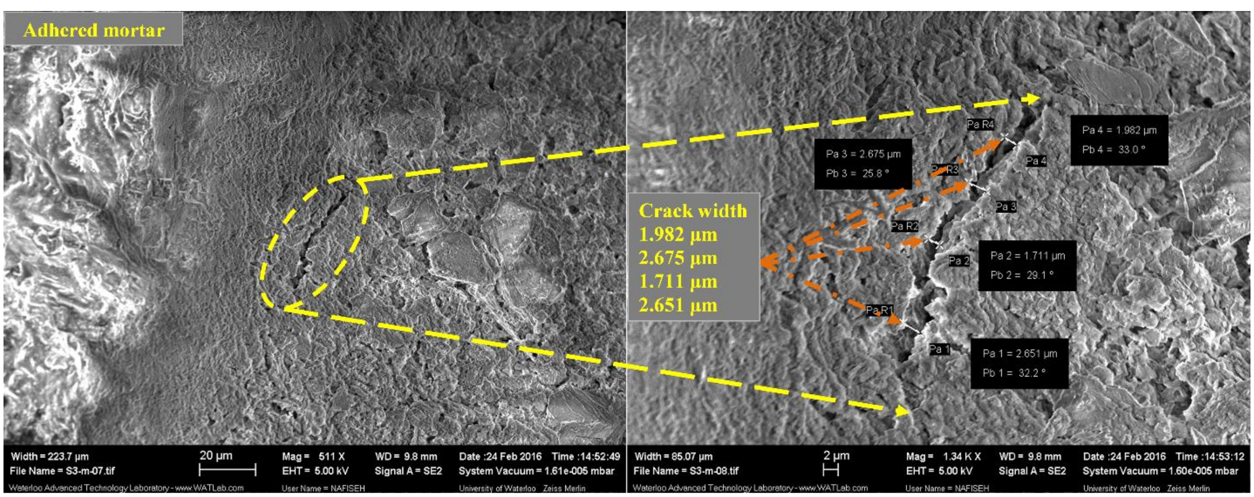

Figure 24: Matrix cracks on mortar surface through HCl treatment

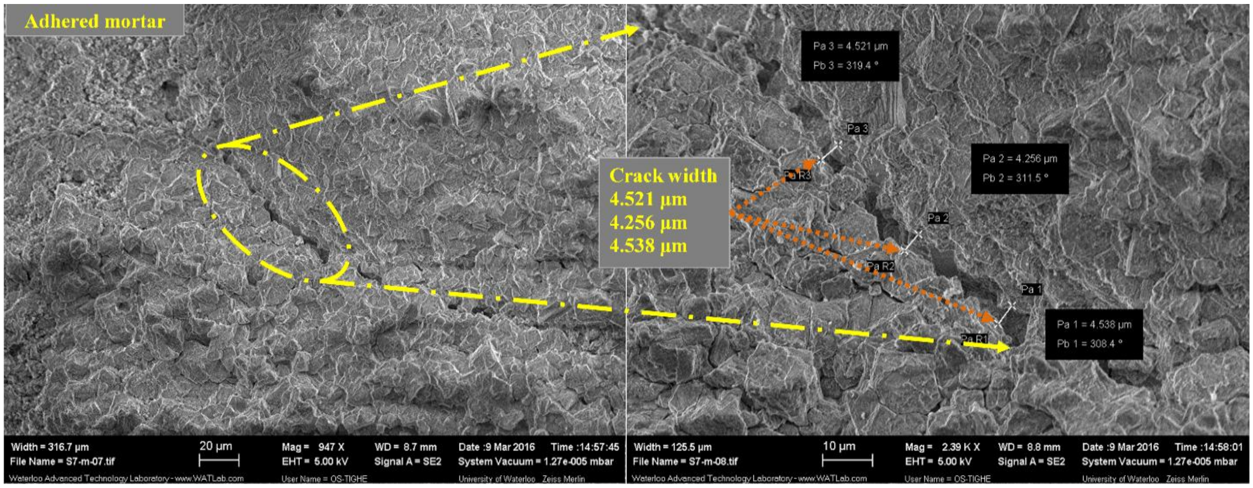

Fig. 25: Matrix cracks on mortar surface through $C_2H_4O_2$ treatment

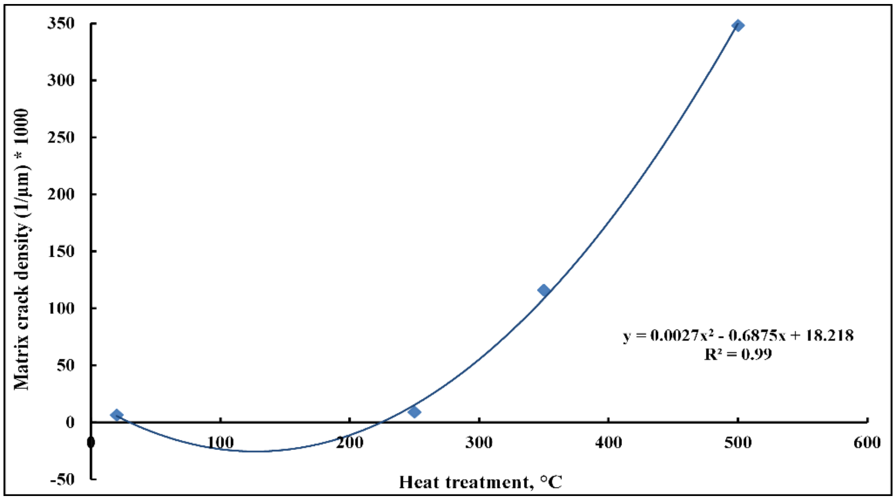

Figure 26: Behavior of matrix crack density through heat treatment

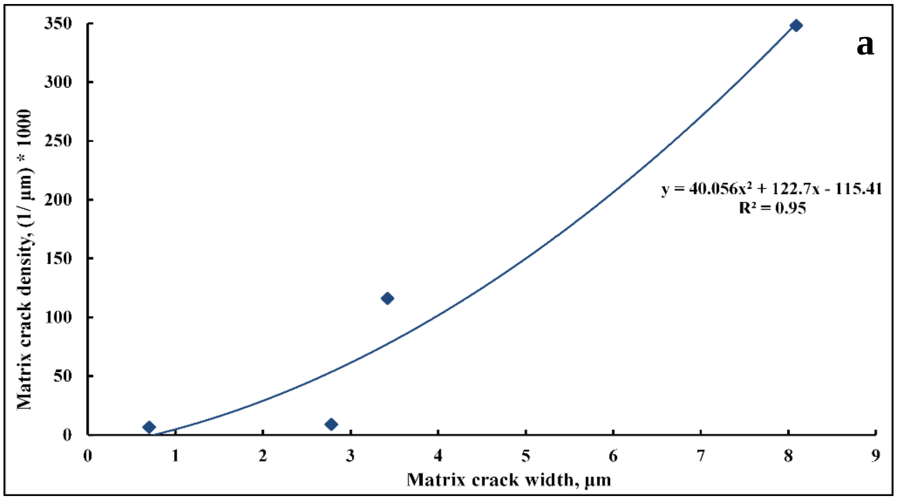

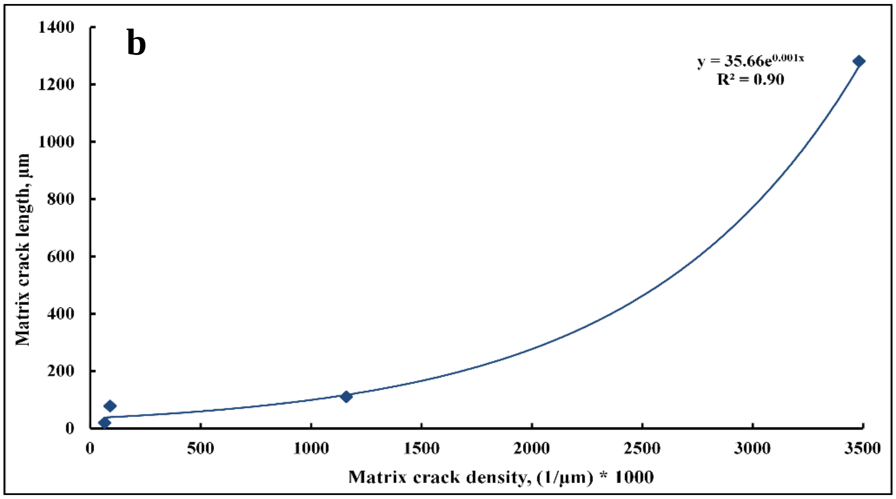

Figure 27: Relationship between matrix crack density and cracks properties:- a: width, b: length

Appendix A: the obtained results of EDAX analysis for aggregate and mortar surface

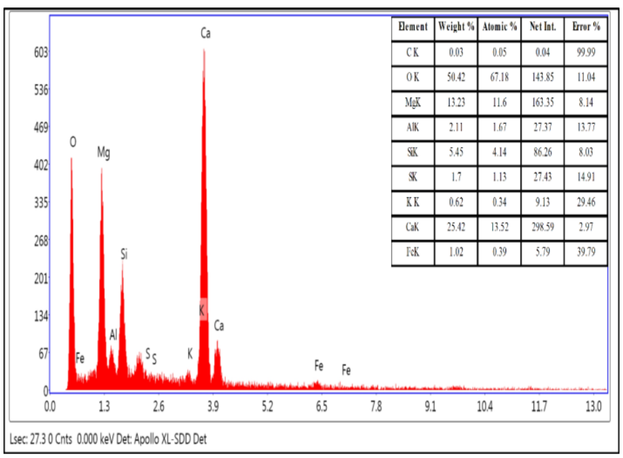

Element	Weight %	Atomic %	Net Int.	Error %
C K	0.03	0.05	0.04	99.99
O K	50.42	67.18	143.85	11.04
MgK	13.23	11.6	163.35	8.14
AlK	2.11	1.67	27.37	13.77
SiK	5.45	4.14	86.26	8.03
SK	1.7	1.13	27.43	14.91
K K	0.62	0.34	9.13	29.46
CaK	25.42	13.52	298.59	2.97
FeK	1.02	0.39	5.79	39.79

Fig. A1-a: EDAX of untreated aggregate surface

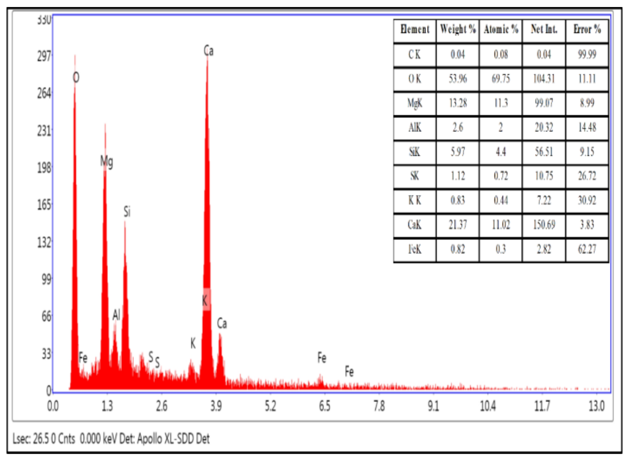

Element	Weight %	Atomic %	Net Int.	Error %
C K	0.04	0.08	0.04	99.99
O K	53.96	69.75	104.31	11.11
MgK	13.28	11.3	99.07	8.99
AlK	2.6	2	20.32	14.48
SiK	5.97	4.4	56.51	9.15
SK	1.12	0.72	10.75	26.72
K K	0.83	0.44	7.22	30.92
CaK	21.37	11.02	150.69	3.83
FeK	0.82	0.3	2.82	62.27

Fig. A1-b: EDAX of aggregate surface at 250°C

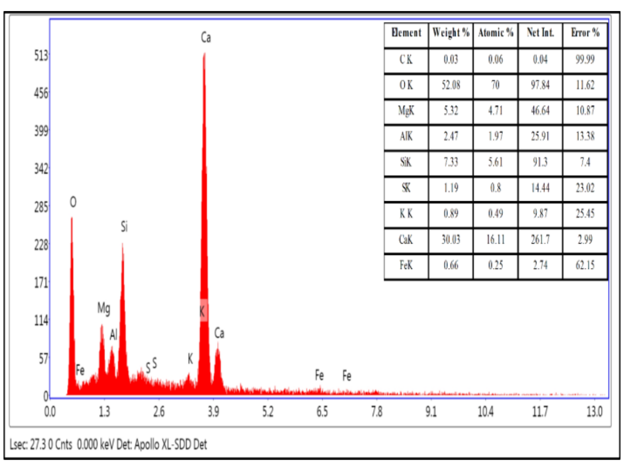

Element	Weight %	Atomic %	Net Int.	Error %
C K	0.03	0.06	0.04	99.99
O K	52.08	70	97.84	11.62
MgK	5.32	4.71	46.64	10.87
AlK	2.47	1.97	25.91	13.38
SiK	7.33	5.61	91.3	7.4
SK	1.19	0.8	14.44	23.02
K K	0.89	0.49	9.87	25.45
CaK	30.03	16.11	261.7	2.99
FeK	0.66	0.25	2.74	62.15

Fig. A1-c: EDAX of aggregate surface at 350°C

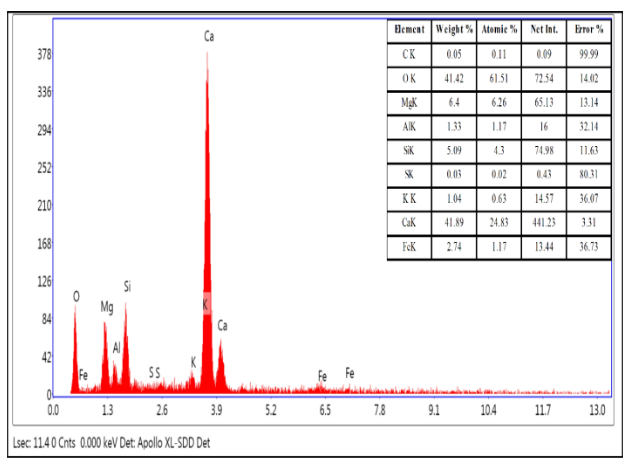

Element	Weight %	Atomic %	Net Int.	Error %
C K	0.05	0.11	0.09	99.99
O K	41.42	61.51	72.54	14.02
MgK	6.4	6.26	65.13	13.14
AlK	1.33	1.17	16	32.14
SiK	5.09	4.3	74.98	11.63
SK	0.03	0.02	0.43	80.31
K K	1.04	0.63	14.57	36.07
CaK	41.89	24.83	441.23	3.31
FeK	2.74	1.17	13.44	36.73

Fig. A1-d: EDAX of aggregate surface at 500°C

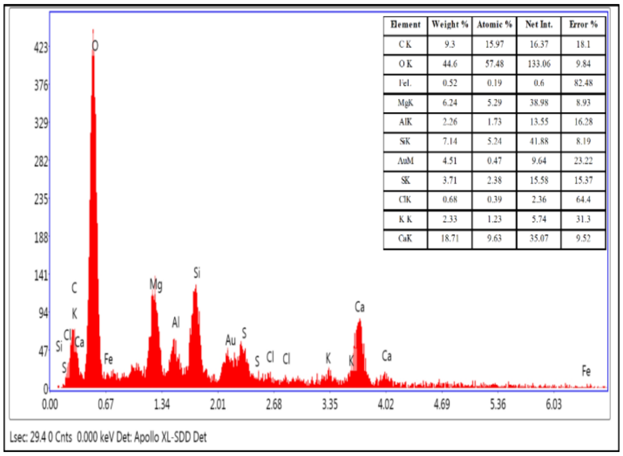

Element	Weight %	Atomic %	Net Int.	Error %
C K	9.3	15.97	16.37	18.1
O K	44.6	57.48	133.06	9.84
FeL	0.52	0.19	0.6	82.48
MgK	6.24	5.29	38.98	8.93
AlK	2.26	1.73	13.55	16.28
SiK	7.14	5.24	41.88	8.19
AuM	4.51	0.47	9.64	23.22
SK	3.71	2.38	15.58	15.37
ClK	0.68	0.39	2.36	64.4
K K	2.33	1.23	5.74	31.3
CaK	18.71	9.63	35.07	9.52

Fig. A1-e: EDAX aggregate surface HCl T.

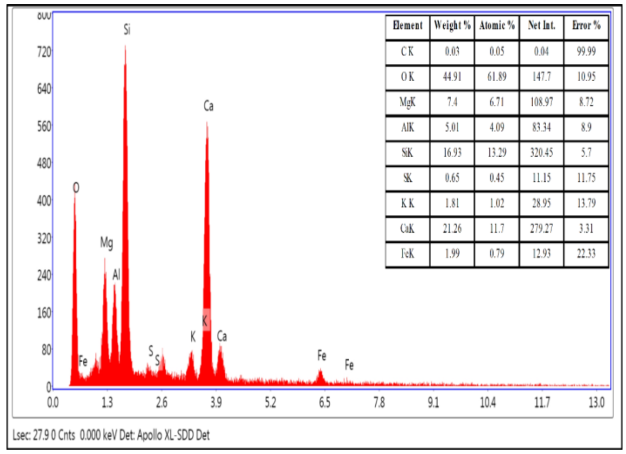

Element	Weight %	Atomic %	Net Int.	Error %
C K	0.03	0.05	0.04	99.99
O K	44.91	61.89	147.7	10.95
MgK	7.4	6.71	108.97	8.72
AlK	5.01	4.09	83.34	8.9
SiK	16.93	13.29	320.45	5.7
SK	0.65	0.45	11.15	11.75
K K	1.81	1.02	28.95	13.79
CaK	21.26	11.7	279.27	3.31
FeK	1.99	0.79	12.93	22.33

Fig. A1-f: EDAX aggregate surface acetic T.

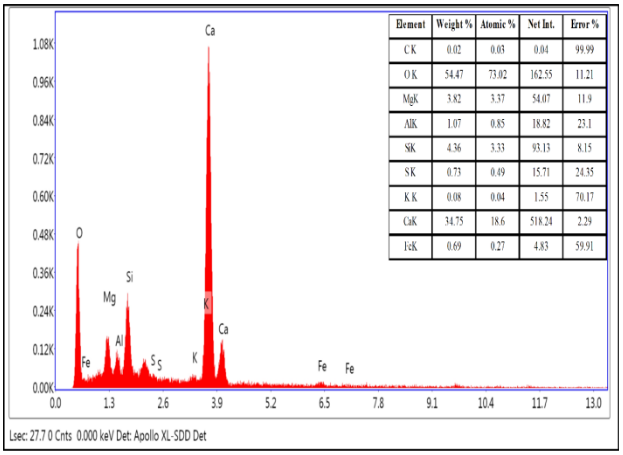

Element	Weight %	Atomic %	Net Int.	Error %
C K	0.02	0.03	0.04	99.99
O K	54.47	73.02	162.55	11.21
MgK	3.82	3.37	54.07	11.9
AlK	1.07	0.85	18.82	23.1
SiK	4.36	3.33	93.13	8.15
S K	0.73	0.49	15.71	24.35
K K	0.08	0.04	1.55	70.17
CaK	34.75	18.6	518.24	2.29
FeK	0.69	0.27	4.83	59.91

Fig. A2-a: EDAX of untreated mortar surface

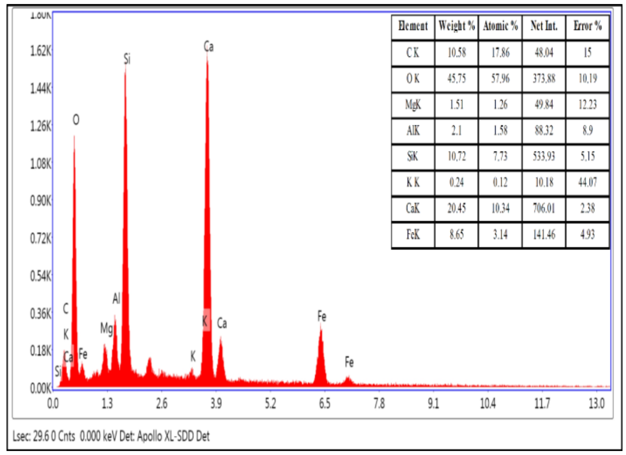

Element	Weight %	Atomic %	Net Int.	Error %
C K	10.58	17.86	48.04	15
O K	45.75	57.96	373.88	10.19
MgK	1.51	1.26	49.84	12.23
AlK	2.1	1.58	88.32	8.9
SiK	10.72	7.73	533.93	5.15
K K	0.24	0.12	10.18	44.07
CaK	20.45	10.34	706.01	2.38
FeK	8.65	3.14	141.46	4.93

Fig. A2-b: EDAX of mortar surface at 250°C

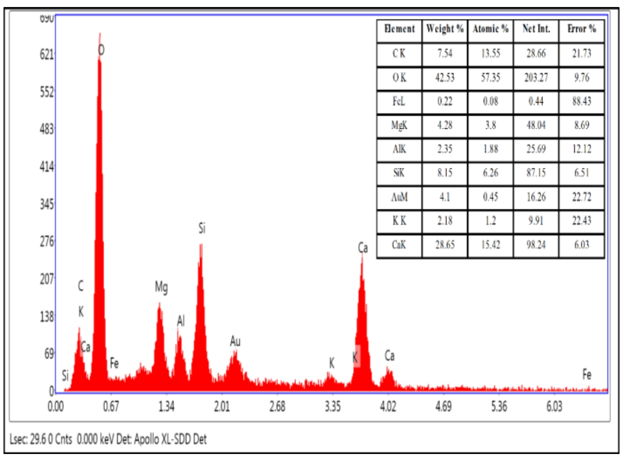

Element	Weight %	Atomic %	Net Int.	Error %
C K	7.54	13.55	28.66	21.73
O K	42.53	57.35	203.27	9.76
FeL	0.22	0.08	0.44	88.43
MgK	4.28	3.8	48.04	8.69
AlK	2.35	1.88	25.69	12.12
SiK	8.15	6.26	87.15	6.51
AuM	4.1	0.45	16.26	22.72
K K	2.18	1.2	9.91	22.43
CaK	28.65	15.42	98.24	6.03

Fig. A2-c: EDAX of mortar surface at 350°C

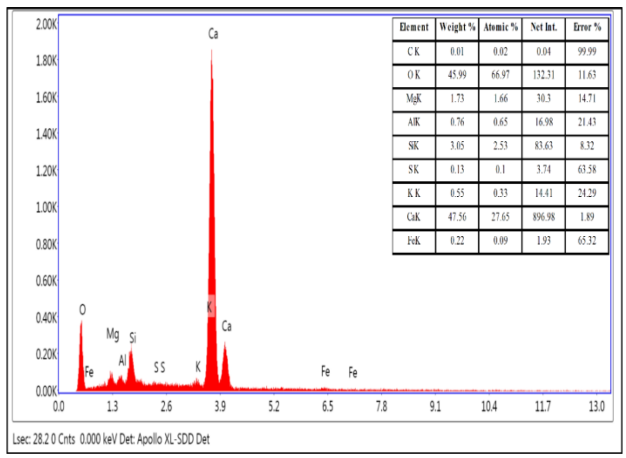

Element	Weight %	Atomic %	Net Int.	Error %
C K	0.01	0.02	0.04	99.99
O K	45.99	66.97	132.31	11.63
MgK	1.73	1.66	30.3	14.71
AlK	0.76	0.65	16.98	21.43
SiK	3.05	2.53	83.63	8.32
SK	0.13	0.1	3.74	63.58
K K	0.55	0.33	14.41	24.29
CaK	47.56	27.65	896.98	1.89
FeK	0.22	0.09	1.93	65.32

Fig. A2-d: EDAX of mortar surface at 500°C

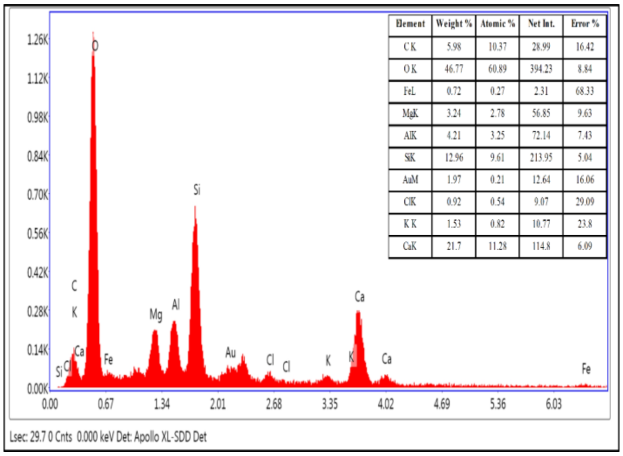

Element	Weight %	Atomic %	Net Int.	Error %
C K	5.98	10.37	28.99	16.42
O K	46.77	60.89	394.23	8.84
FeL	0.72	0.27	2.31	68.33
MgK	3.24	2.78	56.85	9.63
AlK	4.21	3.25	72.14	7.43
SiK	12.96	9.61	213.95	5.04
AuM	1.97	0.21	12.64	16.06
ClK	0.92	0.54	9.07	29.09
K K	1.53	0.82	10.77	23.8
CaK	21.7	11.28	114.8	6.09

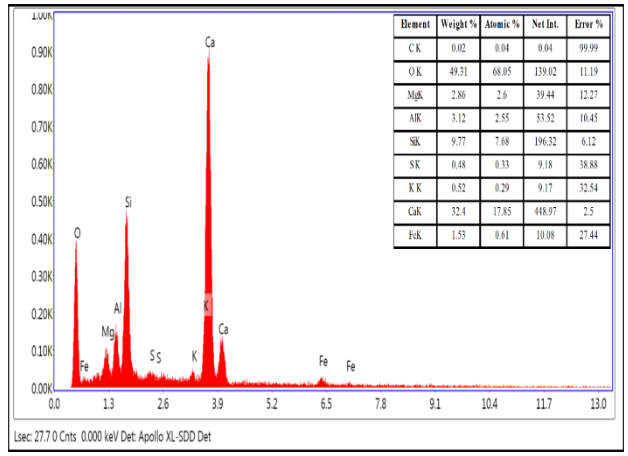

Element	Weight %	Atomic %	Net Int.	Error %
C K	0.02	0.04	0.04	99.99
O K	49.31	68.05	139.02	11.19
MgK	2.86	2.6	39.44	12.27
AlK	3.12	2.55	53.52	10.45
SiK	9.77	7.68	196.32	6.12
S K	0.48	0.33	9.18	38.88
K K	0.52	0.29	9.17	32.54
CaK	32.4	17.85	448.97	2.5
FeK	1.53	0.61	10.08	27.44

Fig. A2-e: EDAX mortar surface HCl treatment Fig. A2-f: EDAX mortar surface acetic treatment